NTNU
Norwegian University of Science and Technology

Investigation of various solutions for improved voltage quality in weak distribution networks

David Fellner

Master of Science in Electric Power Engineering
Submission date: June 2018
Supervisor: Kjetil Uhlen, IEL
Co-supervisor: Wolfgang Gawlik, Vienna University of Technology

Norwegian University of Science and Technology
Department of Electric Power Engineering

Problem Description

Keeping voltages in acceptable limits is a challenge for every grid operator and utility, especially in weak rural distribution networks and on the end of feeders. In rural parts of the grid farms are predominant. These show varying loads especially when starting motors which can lead to problems with assuring voltage stability. The resulting fluctuations in voltage are very undesirable for customers as they can lead to inconveniences as flickering lights or also shorten the lifespan of appliances. The local utility TrønderEnergi is facing issues operating rural distribution grids and is therefore looking for solutions to improve the performance of the grid. These solutions are preferably easy to implement, durable and cost efficient.

The purpose of this thesis is to examine different solutions to the issues mentioned above. In order to do this *MATLAB*® *Simulink*® *Simscape*® models will be developed and data gathered for parameterizing these models. Simulations of critical scenarios will be run to examine the impact of the solutions developed.

Acknowledgments

This thesis was conducted during an ERASMUS exchange semester at the Norwegian University of Science and Technology for the Department of Electric Power Engineering and in collaboration with the local utility TrønderEnergi.

I would very much like to thank my supervisor Professor Kjetil Uhlen for his support, both academically and as an exchange student, which made my stay here surprisingly easy. In addition, I would like to thank TrønderEnergi for their cooperation and providing the grid data as well as the measurements.

I am very grateful to all the friends I made here in Trondheim, for their support and the experiences shared. Especially I am grateful to Adrien Karoui. The parallel development of our work was a great help to me.

Finally, I would like to express my gratitude towards my girlfriend Kira Abstiens who has been very supportive during my stay abroad. I am especially grateful to my brother Klaus who has always provided me with advice and guidance throughout my life. Mostly I would like to thank my parents for all the efforts they made to enable me to accomplish everything I have during the last quarter of a century.

Trondheim, June 2018

David Fellner

Abstract

Voltage instability and low short circuit capacity are a main issue for utilities when operating weak, mostly rural, distribution grids. Especially voltage dips caused by start-ups of induction motors, which are frequently found in rural grids, are problematic. This thesis is investigating several solutions to improve voltage stability and the short circuit capacity of distribution networks like these.

In order to do so electric machines are added to the grid and their impact is analysed. First a realistic grid is modelled using actual data provided by a utility and two induction machine models are implemented. In addition to the induction machine an electrically excited synchronous machine, a PMSM and an additional flywheel linked to the machines are examined as solutions as well. Typical parameters are chosen for all parts of the model. Finally, a start-up of an induction machine and a short circuit simulation is conducted, and the results are discussed.

The conclusion drawn is the induction machine including a flywheel solution showing the best performance in an increased load scenario, as well as in a fault case. It provides voltage support both at the transformer bus and at a local load for a limited time and especially for the transient time frame. Only the big short circuit currents fed into the fault by the induction machine including the flywheel pose a disadvantage regarding protection schemes.

All simulations and modelling is done in $MATLAB^{®}$ $Simulink^{®}$ $Simscape^{®}$.

Contents

Problem Description **i**

Acknowledgments **ii**

Abstract **iii**

Contents **iv**

1 Introduction **1**

1.1 Background 1

1.2 Scope of the work 1

1.3 State of the art 2

2 Grid Model **4**

2.1 System Topology 4

2.2 Line Model 6

2.3 Load Model 6

2.4 Transformer Model 7

2.5 Reactive Power Compensation 7

3 Induction Machine Model **9**

3.1 Park-transformation 9

3.2 Base Model 10

3.3 Model for representation in stability studies 12

3.4 Load Torque Model 13

4 Synchronous Machine Model **14**

4.1 PMSM 14

4.2 Electrically excited SM 16

5 Method **19**
5.1 Grid Model 19
5.2 Induction Machine 19
5.3 PMSM 21
5.4 Electrically excited SM 22
5.5 Flywheel 22
5.6 Compensation tuning 23
5.7 Measurements 24
5.8 Simulations 24

6 Results **27**
6.1 Comparison of the Induction Machine Models 27
6.1.1 Motor Start-up 27
6.1.2 Short Circuit 29
6.1.3 Conclusion 32
6.2 Comparison of Flywheel size 32
6.2.1 Motor Start-up 32
6.2.2 Short Circuit 35
6.2.3 Conclusion 40
6.3 Comparison of Induction Machine and Synchronous Machines 41
6.3.1 Motor Start-up 41
6.3.2 Short Circuit 44
6.3.3 Conclusion 48

7 Discussion **49**
7.1 Discussion 49
7.2 Conclusion 51
7.3 Further work 51

Bibliography **53**

1 Introduction

This chapter gives an outline of the topic, aims and the scope of this work. In addition, a short state of the art is presented.

1.1 Background

Voltage stability is a particularly big issue in rural distribution networks. These grids tend to be weak and have low short circuit capacities. Therefore, especially on the end of feeders, voltage dips caused by load increases can become troublesome. In rural areas a considerable number of customers are farms which use different appliances from usual households. Most farmers conduct wood works and process the wood, if not even run a sawmill. For these purposes induction machines are commonly used. These are started and turned off frequently as turning off the machine is economical for breaks of more than 10 seconds. [1] So especially in a non industrial context frequent voltage dips when motors are started are to be expected making improvements desirable.

1.2 Scope of the work

In this thesis different solutions to improve voltage stability are simulated in a realistic low voltage grid. These are two different induction machine models, an electrically excited synchronous machine, a PMSM and an additional flywheel at the machines.
At first in chapter 2 this distribution grid is modelled in $MATLAB^{®}$ $Simulink^{®}$ $Simscape^{®}$ using information of a local utility. For unspecified parts of the grid assumptions were made that are in line with solutions most commonly used in low voltage distribution grids.
In chapter 3 two different models of induction machines were implemented. As the machines differ in complexity both models are depicted with their sets of equations. In addition, a

load torque model is presented.
Chapter 4 introduces the synchronous machines examined as possible solutions. The choice of machines is briefly outlined as is their functionality and the models used, which are the *Simscape*® built-in ones.
In chapter 5 the parameters for the models used are specified. Also, the implementation and parameterization of an additional flywheel linked to the machines is presented. Moreover, the induction machine model is validated using the built-in model and the compensation is tuned. The simulations conducted are illustrated as well.
Chapter 6 presents the results of the motor start-up and short circuit simulations made and interpreted in detail. In chapter 7 finally these results are discussed, compared and a recommendation on a solution is given. Furthermore, measurements of a field test are presented and compared to the simulation results. Lastly and outlook on possible further work is given.

1.3 State of the art

In several publications the need and solutions for voltage control have been explained, proposed and tested. As described in [2], voltage stability is the ability of a power system to maintain acceptable voltages under normal conditions and when facing disturbances. Voltage instability can occur when not enough reactive power can be supplied. Moreover, little research has been done in regard to distribution systems in comparison to transmission systems.
Following [3], modelling the characteristics, also the dynamic ones, of the induction machine load is important to transient stability. Here this is done with respect to a power system with a large amount of photo voltaic energy generation. It is pointed out that the slip of the induction machine alters during faults, which stands in close relation to the voltage.
[4] suggests a flywheel induction motor as a low-technology solution for a voltage sag compensator. No converters are used in order to keep cost low and avoid harmonics. This solution is found to be simple and highly reliable. It is not being tested on a true-to-life grid though.
In [5] a flywheel energy storage system with a permanent magnet synchronous machine is considered. Here a flywheel is accelerated and stores energy from the network, which it then feeds back to the grid through the PMSM. This was done in connection with a variable speed wind generator, but once again not in connection with a realistic grid. This is stated to be generally considered sufficient to improve the electric power quality.
Finally, [6] points to an improvement of power quality due to the inclusion of a synchronous machine. An enhanced performance during dynamic analysis is obtained, influencing the

reliability and voltage profile if a distribution system favourably. Unlike the system analysed here, the grid is a medium voltage distribution network. Optimal placement of the synchronous machine is also found to have a significant impact on the potential improvement provided by the solution.

Concerning faults [7] looks at the problem of protection blinding in a very weak network environment. This phenomenon occurs when a fault is fed current in parallel by the substation and a distributed generation, which are four synchronous machines in the example case presented. Its pointed out that blinding is always observed to some extent, mostly depending on the fault location and the machine location.

2
Grid Model

In this chapter a model of a low voltage distribution grid is developed. The focus is put on depicting a grid as close to reality as possible. Data of a local utility was used to fulfil this requirement.

2.1 System Topology

The grid modelled is depicted by figure 2.1 and is an actual low voltage distribution network in a rural area of Norway. The local utility TrønderEnergi provided the grid setup [8], which was anonymised, and power flow data for this purpose.
The grid consists of a distribution transformer, 26 buses and 9 loads on 3 feeders. Most of the data for the transformer, the loads and lines was provided by the utility. For not known specifications examples and as near-to-life values were found through literature research. Using all this information fitting models for the parts of the grid were found.

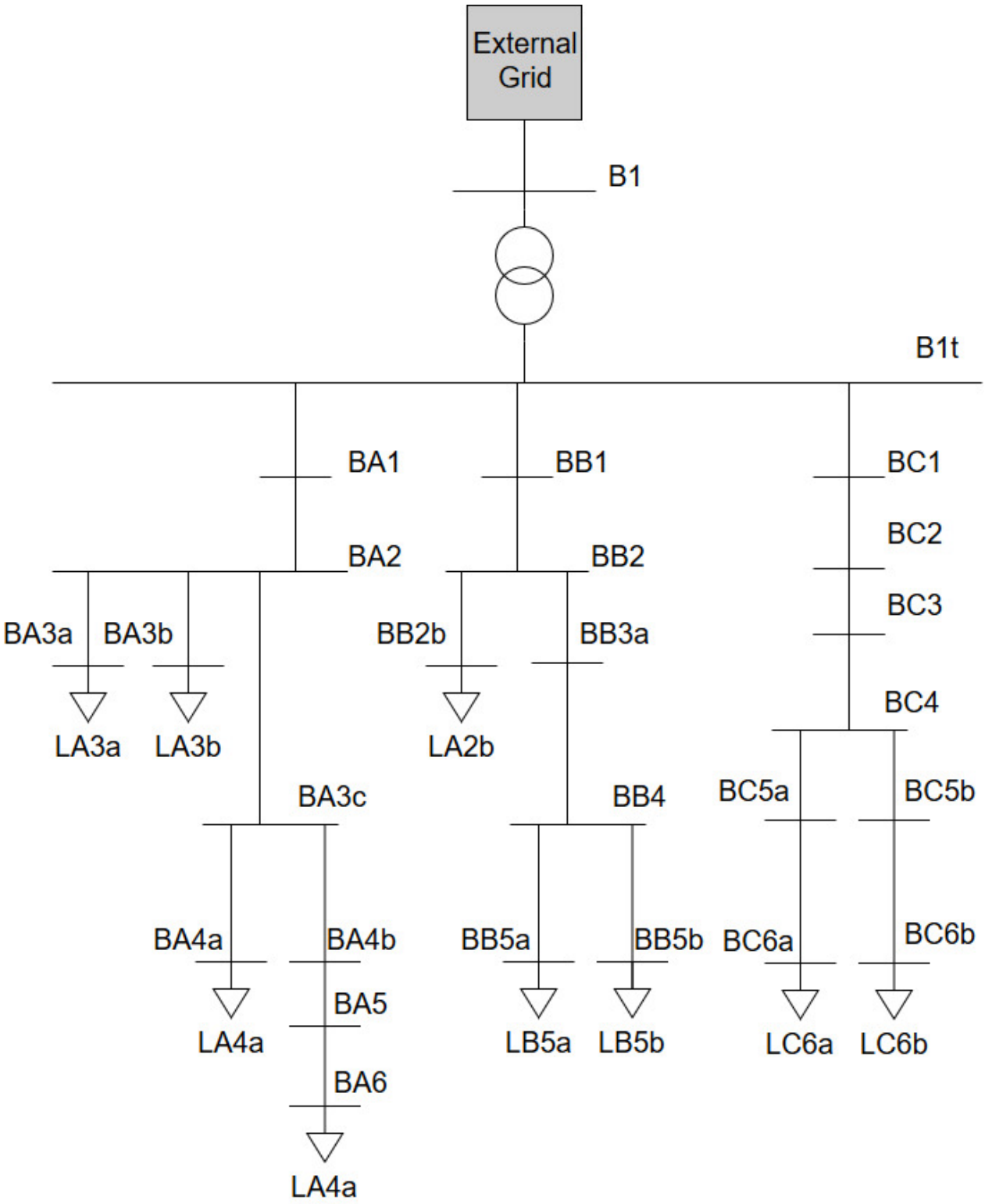

Figure 2.1: Grid Topology

2.2 Line Model

The line model used is the *MATLAB*® *Simulink*® *Simscape*® built in transmission line block. [9]. The model is a lumped-parameter pi-line model.
Figure 2.2 shows the model in symmetrical components:

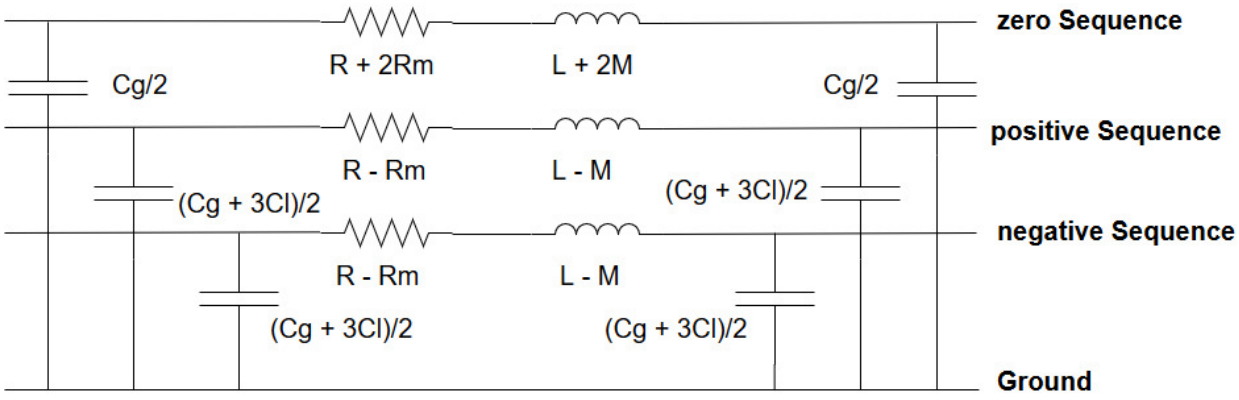

Figure 2.2: Transmission Line Model

The parameters used are:

R	Line resistance
R_m	Mutual resistance
L	Line inductance
C_g	Line-ground capacitance
C_l	Line-line capacitance

2.3 Load Model

The load model is the built in *MATLAB*® *Simulink*® *Simscape*® Wye-Connected load block. [9].
The load consists of a resistor and a inductor connected in series. The parameters are specified by rated power, which is obtained from the power flow calculation provided by the utility. This is done through dividing the actual power consumed by the per unit voltage at the busbar. All reactive powers were assumed to be inductive reactive powers, as these are dominant in domestic appliances. [10]

2.4 Transformer Model

The transformer model is the built in *MATLAB*® *Simulink*® *Simscape*® Wye-Delta11 Transformer block. [9]. The Delta vector group is connected to the high voltage side, whereas the Wye group has a grounded neutral and is connected to the low voltage side. This transformer vector group and set up was chosen since it is well suited for distribution transformers, for it allows to put the full load on the neutral point. [11]
The parameters for distribution transformer of the rural grid were gained from the data provided by TrønderEnergi and specifications from [12]:

S	Rated apparent power	100	kVA
$R_{\sigma 1}$	Primary leakage resistance	0.0088	p.u.
$X_{\sigma 1}$	Primary leakage reactance	0.021	p.u.
$R_{\sigma 2}$	Secondary leakage resistance	0.0088	p.u.
$X_{\sigma 1}$	Secondary leakage reactance	0.021	p.u.
R_s	Shunt magnetizing resistance	500	p.u.
X_s	Shunt magnetizing reactance	500	p.u.

2.5 Reactive Power Compensation

As an electric machine without load also consumes power due to losses and therefore causes a decreased voltage, a reactive power compensation will be added in the grid. The model approach follows the machine connection to the bus-bar in [13]. A line impedance and resistance at the connection to the bus-bar is assumed, as well as a capacitor bank on the line for reactive power compensation. Reactive power is needed by the induction machine for magnetization. A model of the reactive power compensation is shown in 2.3:

This model is described by the following set of equations:

$$\begin{aligned} v_c &= v_a - i_2 r_2 + \frac{di_2}{dt} l_2 \\ \frac{dv_c}{dt} &= i_c \frac{1}{C_a} \\ i_2 &= i_a + i_c \end{aligned} \tag{2.1}$$

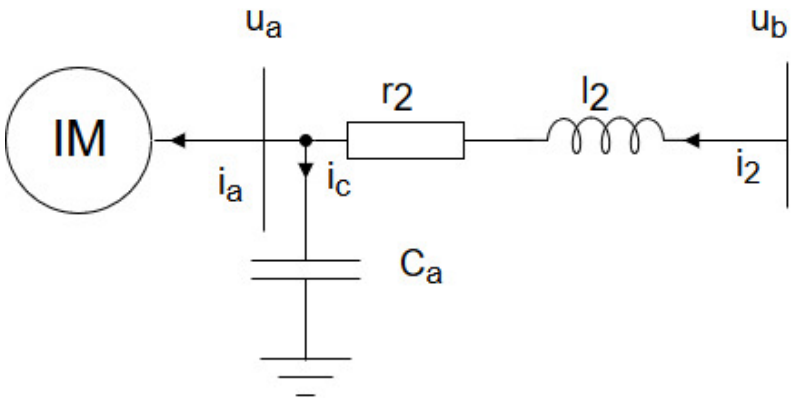

Figure 2.3: Reactive Power Compensation

3

Induction Machine Model

This chapter will introduce the induction machine models used. The models differ in their degree of accuracy, and therefore their behaviour. Especially transient behaviour is going to be of special interest.

3.1 Park-transformation

As in [13] the models used here are based on the Park-transformation. Hereby all armature variables are being transformed to a rotating reference frame which consists of a direct and a quadrature axis that is defined as in [14]:

$$f'_{qd0} = K_s f'_{abc} \tag{3.1}$$

where

$$K_s = \frac{2}{3}\begin{bmatrix} cos(\theta) & cos(\theta - \frac{2\pi}{3}) & cos(\theta + \frac{2\pi}{3}) \\ sin(\theta) & sin(\theta - \frac{2\pi}{3}) & sin(\theta + \frac{2\pi}{3}) \\ \frac{1}{2} & \frac{1}{2} & \frac{1}{2} \end{bmatrix} \tag{3.2}$$

and

$$\omega = \frac{d\theta}{dt} \tag{3.3}$$

from which the relation between the angular velocity, ω, and the angular displacement, θ, can be derived as:

$$\theta = \int \omega dt \tag{3.4}$$

Figure 3.1 depicts the trigonometrical relations between the transformed variables [14]:

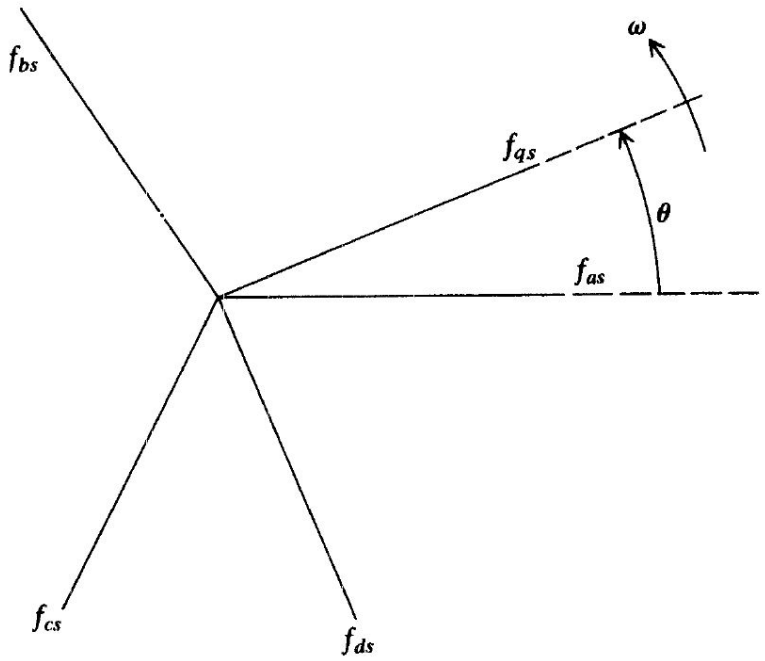

Figure 3.1: dq-reference frame

The Park-Transformation is used both on the armature voltages and currents of the induction machine.

3.2 Base Model

The first model approach is following the induction machine model in [15]. Here the machine is assumed to be cylindrical with short circuited rotor windings. The following equations describe the Base Model in the dq-reference frame:

$$
\begin{aligned}
v_{ad} &= r_s i_{ad} - w_s \Phi_{aq} + \frac{d\Phi_{ad}}{dt} \\
v_{aq} &= r_s i_{aq} + w_s \Phi_{ad} + \frac{d\Phi_{aq}}{dt} \\
v_{a0} &= r_s i_{a0} + \frac{d\Phi_{a0}}{dt} \\
0 &= r_r i_{rq} + \frac{d\Phi_{rq}}{dt} + (w_s - w_a)\Phi_{rd} \\
0 &= r_r i_{rd} + \frac{d\Phi_{rd}}{dt} - (w_s - w_a)\Phi_{rq}
\end{aligned}
\tag{3.5}
$$

$$
\begin{aligned}
\Phi_{aq} &= l_s i_{aq} + l_m i_{rq} \\
\Phi_{ad} &= l_s i_{ad} + l_m i_{rd} \\
\Phi_{a0} &= l_s i_{a0} \\
\Phi_{rq} &= l_m i_{aq} + l_r i_{rq} \\
\Phi_{rd} &= l_m i_{ad} + l_r i_{rd}
\end{aligned}
$$

The torque is characterized by:

$$T_a = \Phi_{rq} i_{rd} - \Phi_{rd} i_{rq} \tag{3.6}$$

and the angular rotor speed by the acceleration equation:

$$\frac{dw_a}{dt} = \frac{1}{2H}(T_a - T_m) \tag{3.7}$$

The variables used express the following properties:

v_{ad}, v_{aq}, v_{a0}	Stator voltage components	[p.u]
i_{ad}, i_{aq}, i_{a0}	Stator current components	[p.u]
w_s	synchronous frequency	[p.u]
w_a	rotational speed of induction machine rotor	[p.u]
Φ_{ad}, Φ_{aq}, Φ_{a0}	Stator flux linkage components	[p.u]
Φ_{rd}, Φ_{rq}	Rotor flux linkage components	[p.u]
r_s, r_r	Stator and rotor resistance	[p.u]
l_s, l_r	Stator and rotor self inductances	[p.u]
l_m	Mutual inductance	[p.u]
T_a	Air gap torque	[p.u]
H	Inertia constant	[s]

3.3 Model for representation in stability studies

As describes in [15] the stator flux derivatives are being neglecting in the stator voltage component equations for representation in power system stability studies. By neglecting these terms, the dc component in the stator transient currents are ignored. This is done to ensure compatibility with other system components as the transmission network. Based on this another reduced model approach is implemented by:

$$\begin{aligned}
v_{ad} &= R_s i_{ad} - w_s \Phi_{aq} \\
v_{aq} &= R_s i_{aq} + w_s \Phi_{ad} \\
u_{a0} &= R_s i_{a0} \\
0 &= r_r i_{rq} + \frac{d\Phi_{rq}}{dt} + (w_s - w_a)\Phi_{rd} \\
0 &= r_r i_{rd} + \frac{d\Phi_{rd}}{dt} - (w_s - w_a)\Phi_{rq}
\end{aligned} \tag{3.8}$$

$$\begin{aligned}
\Phi_{aq} &= l_s i_{aq} + l_m i_{rq} \\
\Phi_{ad} &= l_s i_{ad} + l_m i_{rd} \\
\Phi_{a0} &= l_s i_{a0} \\
\Phi_{rq} &= l_m i_{aq} + l_r i_{rq} \\
\Phi_{rd} &= l_m i_{ad} + l_r i_{rd}
\end{aligned}$$

As above the torque and angular rotor speed are defined as:

$$T_a = \Phi_{rq} i_{rd} - \Phi_{rd} i_{rq} \tag{3.9}$$

$$\frac{dw_a}{dt} = \frac{1}{2H}(T_a - T_m) \tag{3.10}$$

using the same variables as listed in the first model.

3.4 Load Torque Model

The load torque varies with speed. A common model, which is also used in this case, for the load torque is

$$T_m = T_0(Aw_a^2 + Bw_a + C) \tag{3.11}$$

with A + B + C = 1. Since these parameters depend on the driven mechanical loads A is generally set to 1, whereas B and C are set to 0. This leaves us with a load torque quadratically proportional to the angular rotor speed, which is often the case for small industrial appliances such as saws. [16]

4

Synchronous Machine Model

This chapter will describe the choice of machine types for the synchronous machine. A brief explanation of the function as well as an overview of the modelling approach used is given.

4.1 PMSM

As suggested in [17] a permanent magnet synchronous machine, called PMSM in the following, is the type of synchronous machine best fit for a flywheel application and therefor chosen for this simulation. The machine is proposed for applications in road vehicles for its efficiency, costs and material limitations.

The PMSM uses permanent magnets instead of an electrical excitation to create the rotor flux. [18] Figure 4.1 depicts the principle build-up of a PMSM with one pole pair:

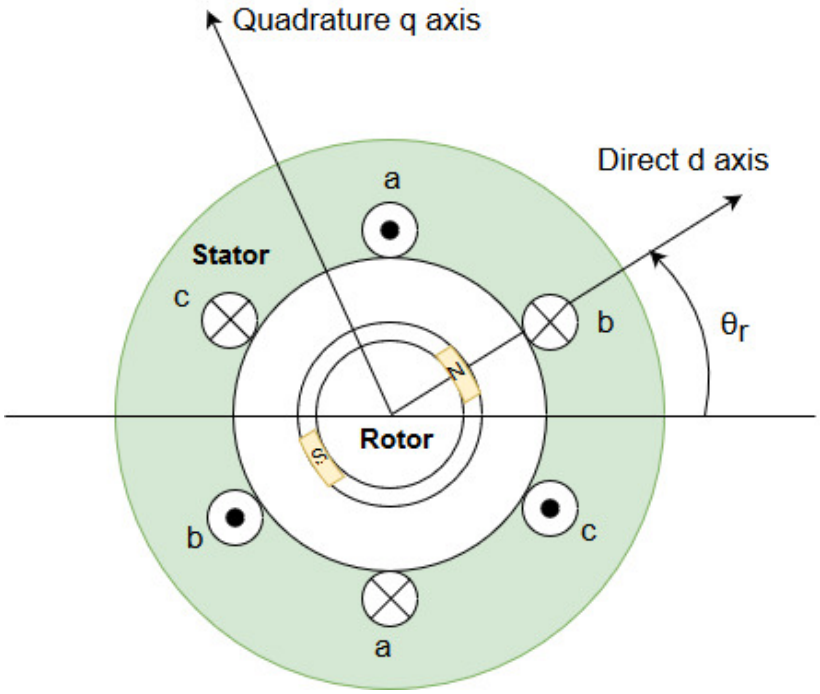

Figure 4.1: PMSM sketch

The model used is the built-in *Simscape*® model in *MATLAB*® *Simulink*®. [9] As for the induction machine Park's transformation is applied, yielding the following equations describing the behaviour of the PMSM:

$$\begin{aligned} v_d &= R_s i_d + L_d \frac{di_d}{dt} - N w i_q L_q \\ v_q &= R_s i_q + L_q \frac{di_q}{dt} + N w (i_d L_d + \Phi_m) \\ v_0 &= R_s i_0 + L_0 \frac{di_0}{dt} \\ T &= \frac{3}{2} N (i_q (i_d L_d + \Phi_m) - i_d i_q L_q) \end{aligned} \tag{4.1}$$

where:

v_d, v_q, v_0	Stator d, q and zero-sequence voltage components
i_d, i_q, i_0	Stator d, q and zero-sequence current components
Φ_m	Permanent magnet flux linkage
R_s	Equivalent resistance of each stator winding
L_d, L_q, L_0	Stator d-axis, q-axis and zero-sequence inductance
w	Rotor mechanical rotational speed
N	Number of rotor permanent magnet pole pairs
T	Rotor torque

The motor is parameterized using the back EMF constant, which is defined as the peak voltage induced by the permanent magnet in each of the phases:

$$k_e = N\Phi_m \tag{4.2}$$

4.2 Electrically excited SM

As the 'standard' synchronous machine is an electrically excited synchronous machine, a machine of this type was used in the simulation as well. This machine serves as a kind of reference to the other stability improvements.
As for the PMSM the built-in *Simscape*® model in *MATLAB*® *Simulink*® is used. The model used is the 'Synchronous Machine Round Rotor (standard)' model. [9] Here 'standard' refers to the parameterization.

The electrically excited synchronous machine is widely used to generate electrical energy. Its stator is built up similar to the induction motors. The rotor in this model is a round and not salient, which is typical for machines with a small number of pole pairs.
The machine is excited by a DC current that can either run through an external exciter generator or through the rotor field windings, which is the case here, to induce the magnetic field. [19]

Also, here the Park's transformation is used to define the machine equations in per-unit:

$$
\begin{aligned}
e_d &= \frac{1}{\omega_{base}} \frac{d\Phi_d}{dt} - \Phi_q \omega_r - R_a i_d \\
e_q &= \frac{1}{\omega_{base}} \frac{d\Phi_q}{dt} - \Phi_d \omega_r - R_a i_q \\
e_0 &= \frac{1}{\omega_{base}} \frac{d\Phi_0}{dt} - R_a i_0
\end{aligned}
\tag{4.3}
$$

for the stator voltages, with:

e_d, e_q, e_0	d, q and zero-sequence voltages
Φ_d , Φ_q, Φ_0	d, q and zero-sequence flux linkages
R_a	stator resistance
w_{base}	per-unit base electrical speed
w_r	per-unit rotor rotational speed
i_d, i_q, i_0	d, q and zero-sequence stator currents

Further the rotor voltages are defined by:

$$
\begin{aligned}
e_{fd} &= \frac{1}{\omega_{base}} \frac{d\Phi_{fd}}{dt} + R_f di_{fd} \\
e_{1d} &= \frac{1}{\omega_{base}} \frac{d\Phi_{1d}}{dt} + R_1 di_{1d} = 0 \\
e_{1q} &= \frac{1}{\omega_{base}} \frac{d\Phi_{1q}}{dt} + R_1 qi_{1q} = 0 \\
e_{2q} &= \frac{1}{\omega_{base}} \frac{d\Phi_{2q}}{dt} + R_2 qi_{1q} = 0
\end{aligned}
\tag{4.4}
$$

using the parameters:

e_{fd}	field voltage
e_{1d}, e_{1q}, e_{2q}	d1, q1 and q2 damper winding voltages
Φ_{fd} , Φ_{1d}, Φ_{1q},Φ_{2q}	magnetic fluxes linking the field circuit, d1, q1 and q2 damper windings
R_{fd} , R_{1d}, R_{1q},R_{2q}	resistances of rotor field circuit, d1, q1 and q2 damper windings
i_{fd} , i_{1d}, i_{1q},i_{2q}	currents flowing in the field circuit, d1, q1 and q2 damper windings

The equations show that the model used is one with one damper winding on the d-axis and two damper windings on the q-axis.

The stator flux linkage equations are defined by:

$$\begin{aligned} \Phi_d &= -(L_{ad} + L_l)i_d + L_{ad}i_{fd} + L_{ad}i_{1d} \\ \Phi_q &= -(L_{aq} + L_l)i_q + L_{aq}i_{1q} + L_{aq}i_{2q} \\ \Phi_0 &= -L_0 i_0 \end{aligned} \tag{4.5}$$

with

L_l	stator leakage inductance
L_{ad}, L_{aq}	d- and q-axis mutual inductances of the stator

The rotor flux linkages equations are:

$$\begin{aligned} \Phi_{fd} &= L_{ffd}i_{fd} + L_{f1d}i_{1d} - L_{ad}i_d \\ \Phi_{1d} &= L_{f1d}i_{fd} + L_{11d}i_{1d} - L_{ad}i_d \\ \Phi_{1q} &= L_{11q}i_{1q} + L_{aq}i_{2q} - L_{aq}i_q \\ \Phi_{2q} &= L_{aq}i_{1q} + L_{22q}i_{2q} - L_{aq}i_q \end{aligned} \tag{4.6}$$

where L_{ffd}, L_{11d}, L_{11q} and L_{22q} are the self inductances of the rotor field and d- and q-axis damper windings. L_{f1d} is the rotor field and d-axis damper winding mutual inductance. The inductances are defined by time constants.

Finally, the rotor torque is defined as:

$$T_e = \Phi_d i_q - \Phi_q i_d \tag{4.7}$$

5 Method

This chapter will introduce the specifications of the grid, machines and measurements used in the simulation and describe the simulated cases.

5.1 Grid Model

The data for the rural distribution grid was provided by TrønderEnergi. The cable data was retrieved from [20]. The external grid, to which the distribution transformer is connected, is modelled as a 50Hz voltage source without any source impedance. This means the external grid is regarded as a stiff network. The voltage source is set to a rated voltage of 21.019kV, which is the value provided by the utilities data.
To validate the power flow data provided by TrønderEnergi a power flow in *MATLAB*® was conducted using matpower [21]. This power flow calculation yields the same voltage levels for the buses and total power consumption of the entire grid as listed in the utilities data and therefore serves as a cross check between the power flow data and the implemented grid model.
The *MATLAB*® *Simulink*® *Simscape*® model of the grid is found at the end of this chapter in Figure 5.5.

5.2 Induction Machine

The induction machine parameters used are obtained from the machine modelled in [13]:

	Parameter	SI units	Per Unit
Stator resistance	r_s	0.018 Ω	0.019
Rotor resistance	r_r	0.019 Ω	0.020
Stator inductance	l_s	8.49 mH	2.774
Rotor inductance	l_r	8.58 mH	2.804
Mutual inductance	l_m	8.17 mH	2.669
Number of poles	n_{poles}	6	-
Induction machine inertia	J	1.40 kgm^2	0.28 s

Table 5.1: Induction machine parameters

These machine specifications were used for the motor being started up as well as for the support machine application. The

The modelling itself was conducted using *MATLAB*® *Simulink*® *Simscape*® and guided by a machine modelling approach in [22].

These specifications were compared to the 'Asynchronous Machine Squirrel Cage (fundamental)' *MATLAB*® *Simulink*® *Simscape*® built-in model for verification. The case examined is a start-up of the motors on an ideal voltage source at 230V and a load torque of 1751 Nm. Figures 5.1 and 5.2 show the speed and torque curves and the active and reactive power consumption of both motors during the start-up and in the steady state after that.

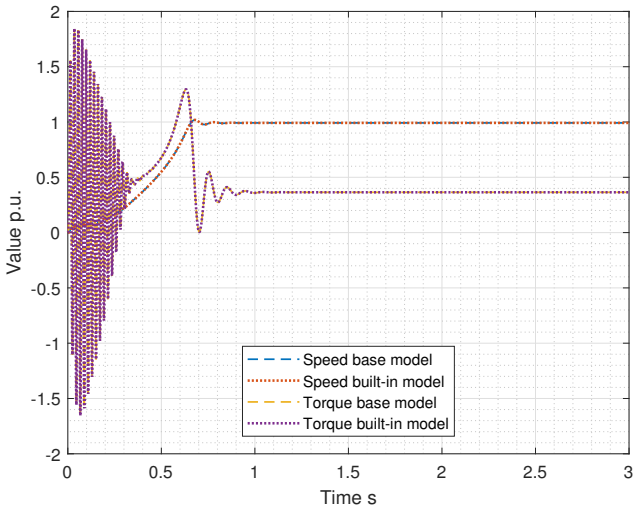

Figure 5.1: Speed and Torque

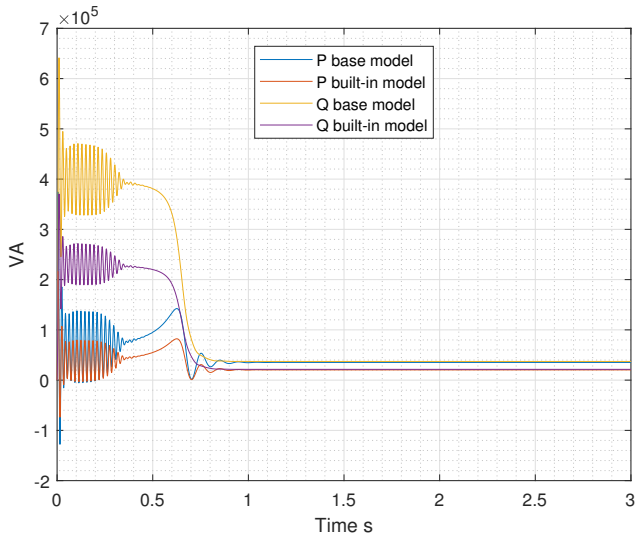

Figure 5.2: Active- and reactive power

Both models have the same start-up time and torque curve, however both active and reactive power consumed by the built-in model are lower than what the base model consumes. This is assumed to be because of the parametrization of the built-in models rated power, which alters the power consumed significantly, but also the start-up time. The base model is only defined by its resistances and reactances so it remains not completely clear where the differences in the models are. Nevertheless, the two models show the same qualitative behaviour and therefore the higher power consumption is looked at as being a conservative model approach and the base model as a valid induction machine model in general.

5.3 PMSM

The parameters for such a machine are gained from [5]:

Stator resistance	R_s	=	0.944 Ω
Direct-axis inductance	L_d	=	14.44 mH
Quadrature-axis inductance	L_q	=	25.06 mH
Back-EMF coefficient	k_e	=	0.78 $Vrad^{-}1$
Number of poles	2p	=	6

Table 5.2: Permanent magnet synchronous machine parameters

In addition the Stator zero-sequence inductance, L_0, was assumed as 1mH following [23].

5.4 Electrically excited SM

The parameters for the electrically excited synchronous machine were obtained from [13], [24] as well as from [25] for a 75kVA machine.

The field circuit voltage of 42V is the voltage necessary to keep the terminal voltage at its rated value at no load. This input also defines the parameters for the field circuit.
Due to lack of time for further implementations the field voltage is provided by the built in ideal DC voltage source providing a voltage of 42V at all times. This can be assumed to be realistic for this voltage could be provided by a backup battery which is always assumed to be charged.

Table 5.3 shows the specifications and parameters used:

Rated apparent power	S_r	=	55 kVA
Rated voltage	V_r	=	400 V
Rated electrical frequency	f_r	=	50 Hz
Number of pole pairs	p	=	2
Field circuit voltage	V_f	=	42 V
Stator resistance	R_a	=	0.01 $p.u.$
Stator leakage reactance	X_l	=	0.15 $p.u.$
d-axis synchronous reactance	X_d	=	1.80 $p.u.$
q-axis synchronous reactance	X_q	=	1.80 $p.u.$
zero-sequence reactance	X_0	=	0.15 $p.u.$
d-axis transient reactance	X'_d	=	0.3 $p.u.$
q-axis transient reactance	X'_q	=	0.65 $p.u.$
d-axis subtransient reactance	X''_d	=	0.19 $p.u.$
q-axis subtransient reactance	X''_q	=	0.19 $p.u.$
d-axis transient open-circuit time constant	T'_{d0}	=	8 s
d-axis subtransient open-circuit time constant	T''_{d0}	=	0.03 s
q-axis transient open-circuit time constant	T'_{q0}	=	1 s
q-axis subtransient open-circuit time constant	T''_{q0}	=	0.07 s

Table 5.3: Electrically excited synchronous machine parameters

5.5 Flywheel

As the induction machine is also implemented with a flywheel, the inertia parameter for this was chosen to be $J = 17.9kgm^2$ as in [4]. This means the flywheel is simply modelled as an extra inertia.

The PMSM is simulated with the same inertia and the same flywheel inertia as the induction machine for reasons of comparability. The electrically excited synchronous machine is just implemented with an inertia of $J = 1.4kgm^2$, but not with the extra inertia of the flywheel.

5.6 Compensation tuning

The capacitance of the compensation was chosen as to restore the voltage at the transformer bus to the level without any flywheel. In Figure 5.3a four cases of a motor start-up are depicted. In the first case without any flywheel hooked to the grid, secondly with the induction machine as a flywheel, thirdly the case with the permanent magnet synchronous machine and finally with the electrically excited synchronous machine linked to the grid.

Following this the capacitance of the compensation was adjusted. By that the voltages at the transformer were lifted to their initial levels:

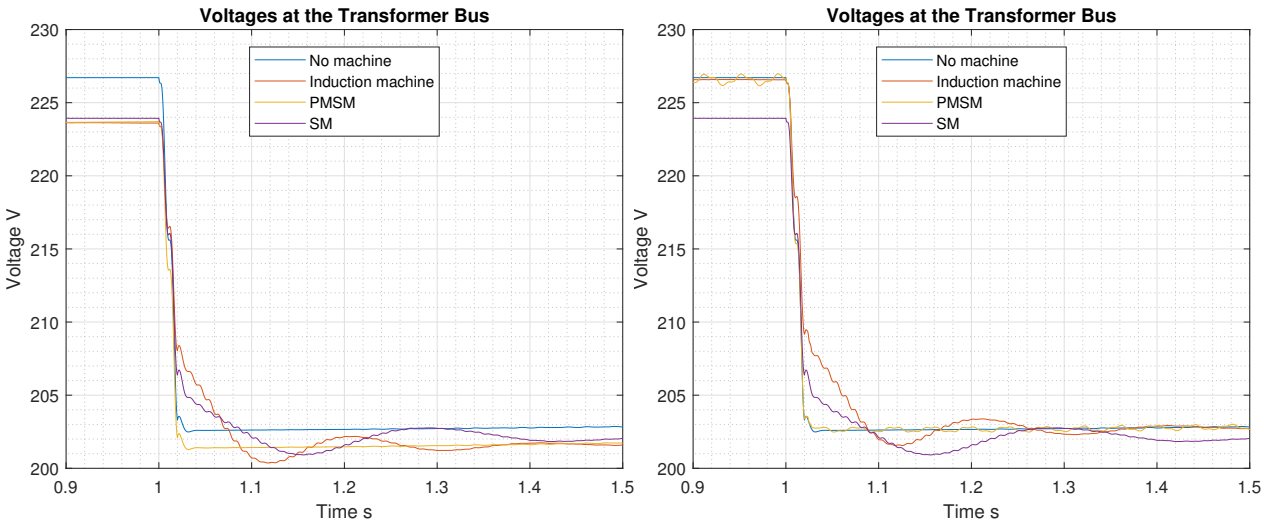

(a) Without compensation

(b) Adjusted compensation

For the induction machine a capacitance of $660\mu F$ was found to be appropriate. For the PMSM a capacitance of $495\mu F$ was chosen. The compensations adds some minor oscillations to the voltage in the when the PMSM is connected to the grid, This is most likely a resonance phenomenon.
There is no compensation applied to the electrically excited synchronous machine.

5.7 Measurements

All measurements are done by a custom *Simscape*® block.
The current and voltage measurements are conducted as RMS measurements using the instantaneous value of phase A since the grid is assumed to be symmetrical:

$$\begin{aligned} V &= \sqrt{\frac{1}{T}\int^{T} v_a^2} \\ I &= \sqrt{\frac{1}{T}\int^{T} i_a^2} \end{aligned} \tag{5.1}$$

The power measurements are carried out instantaneously following [26]:

$$\begin{aligned} P &= v_a i_a + v_b i_b + v_c i_c \\ Q &= \frac{1}{\sqrt{3}}[(v_b - v_c)i_a + (v_c - v_a)i_b + (v_a - v_b)i_c] \end{aligned} \tag{5.2}$$

where v_{abc} and i_{abc} represent the phase properties of the voltage and current.

5.8 Simulations

All simulation are done in *MATLAB*® *Simulink*® *Simscape*® using a solver of the type Backward Euler with a sample time of $10^{-5}s$. This sample time was chosen due to the occurrence of oscillations at higher sample times. *Simscape*® was chosen since it is more fit to model physical systems in comparison to causal modelling, which is represented by *Simulink*® on its own. [27]
Two cases are being simulated: a motor start-up and a short circuit. Both are simulated under various conditions. Firstly, without any further measures to improve voltage stability to have a general reference. Then both induction machine models (the full model and the model neglecting stator flux derivatives), the PMSM and finally the Synchronous machine are linked to the grid in order to study their impact on voltage stability and short circuit currents. In addition to that different values of inertia are implemented to simulate the impact of a flywheel added to a motor.
All the machines used for voltage stability improvement studies are connected to bus BB5b and are running at their nominal rotational speed as the motor start-up or short circuit takes place.

To simulate a motor start-up the induction motor model presented above is linked to bus

BB5a of the grid, so at the very end of the feeder. The motor is started with a load torque of 1575.9 Nm.

The short circuit is simulated as a three-phase short circuit between the buses BB2 and BB2b. For this the *MATLAB*® *Simulink*® *Simscape*® [9] built-in short circuit model is used.
A resistance of 0.5 Ω was chosen following an approximation in [28]. The resistance is understood as a phase-to-ground resistance and therefore split up equally between the phase-to-neutral resistances R_a, R_b and R_c and the neutral-to-ground resistance R_g. These are connected in series as Figure 5.4 shows:

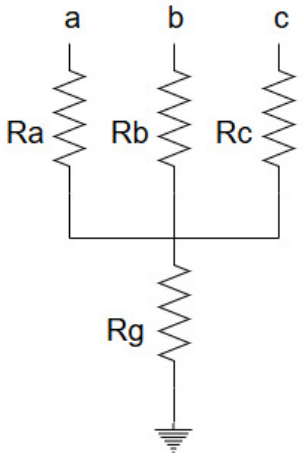

Figure 5.4: 3 phase short circuit model

The short circuit is cleared after 100ms by opening a circuit breaker disconnecting the feeder of the load LA2b at the bus BB2.

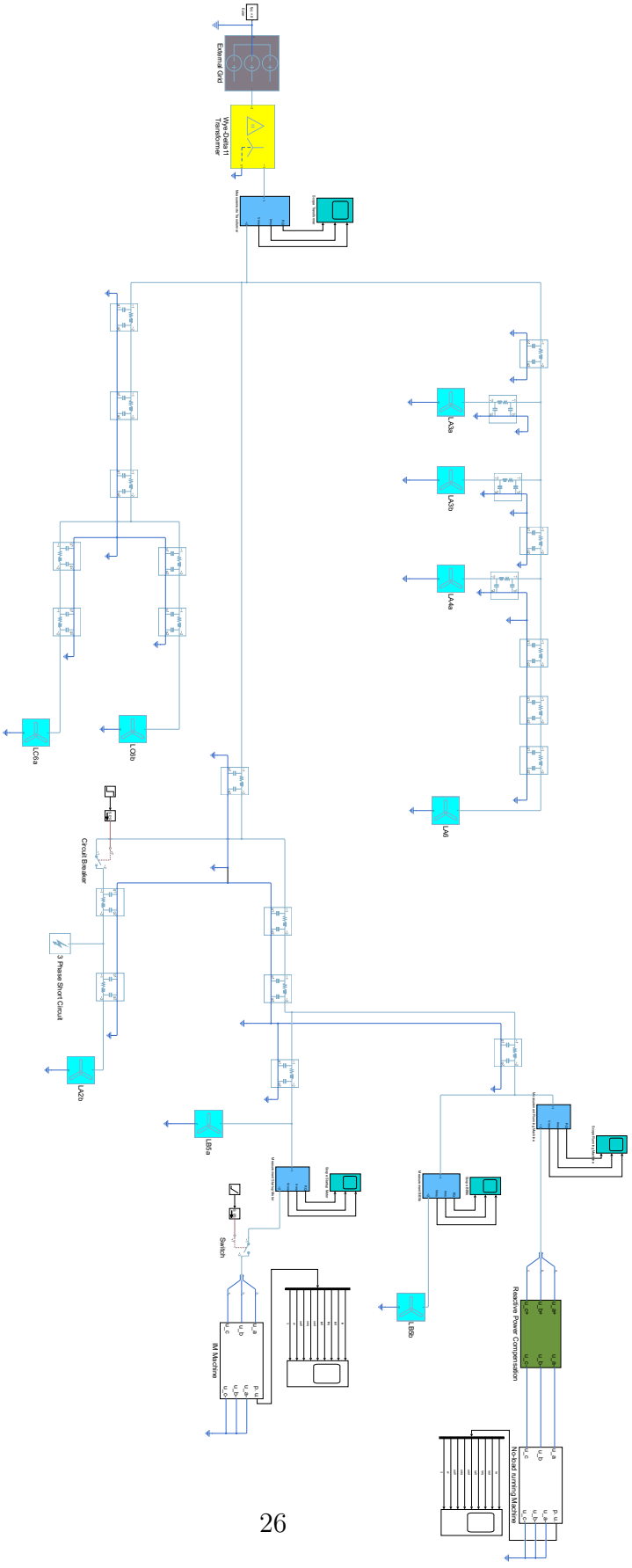

Figure 5.5: Model of the Grid in *MATLAB*® *Simulink*® *Simscape*®

6 Results

This chapter will present and analyse the results of both the motor start-up and short circuit simulation cases with respect to the different additions made to the grid. These include the different types of electrical machines and the flywheel.

6.1 Comparison of the Induction Machine Models

Firstly, the two implemented induction motor models are compared in the motor start-up and the short circuit scenario. It is going to be of special interest what impact the less accurate depiction of the transient behaviour that the neglect of the stator flux derivatives brings has.

6.1.1 Motor Start-up

Figure 6.1 shows the voltage at bus BB5a and therefor the voltage at a local load close to the machine being started up. The induction machine base model for the supporting machine bolsters the voltage at this local load better than the model neglecting stator flux derivatives right after the motor start-up. The deepest voltage dip is avoided due to this.
In figure 6.2, showing the power at the supporting machine, the reason for this behaviour becomes obvious: in the very first instant the reactive power provided by the base model machine is bigger than what the reduced model machine provides. The energy stored in the stator flux is contributing to the power set free by the base model machine allowing it to provide more power.
After the first 50ms the two machines behave very similar and therefore their impact on the voltage at the local load is the same as well: both add oscillation to the voltage lifting the voltage up at first.

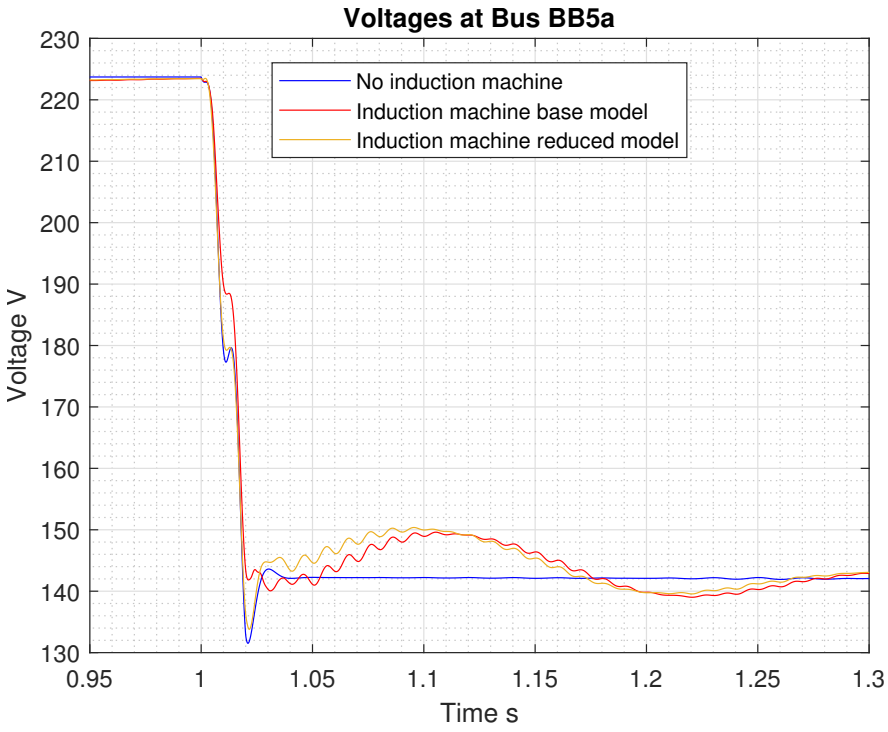

Figure 6.1: Comparison of Voltages at Bus BB5a

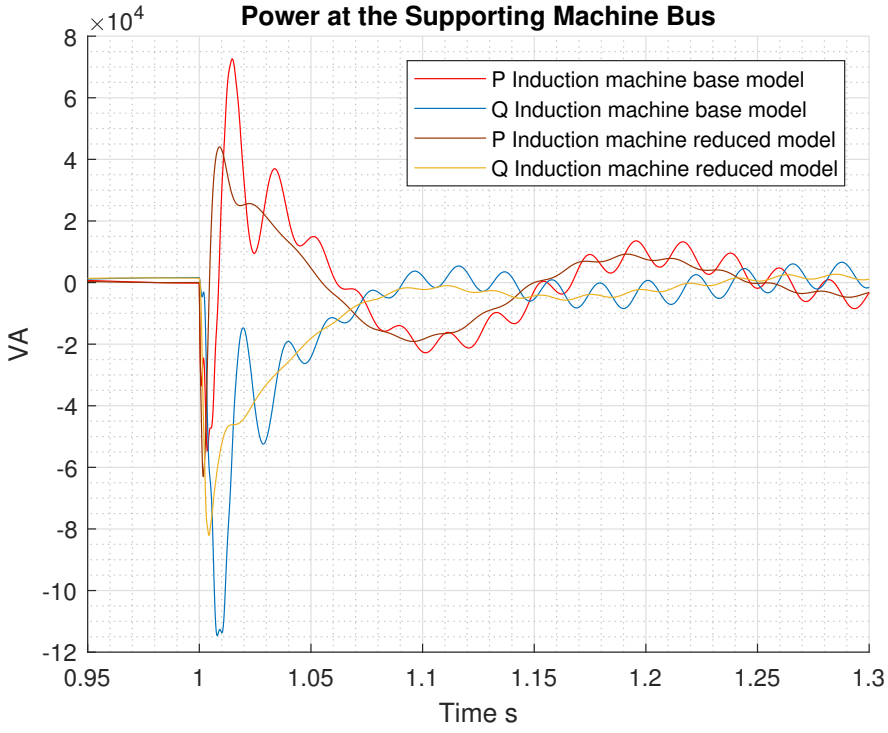

Figure 6.2: Comparison of Power at the Supporting Machine Bus

6.1.2 Short Circuit

In figure 6.3 the voltage at the transformer bus is shown. Both induction machine models show very similar responses: they lift the voltage for the first half of the duration of the short circuit. After this the voltage level falls below the level of the case without a supporting machine connected. The full model of the induction machine provides a voltage curve that is a little lower than the one of the reduced model.
Figure 6.4 once more shows why this is the case: both machine models provide less energy as the short circuit goes on. At a certain point power consumption outweighs the power provided. The supporting machine decelerates, making it impossible to feed power back into the grid. The only notable difference between the two models is the instantaneous response of the model neglecting the stator flux derivatives in comparison to a delayed response of the full model. The stator flux derivatives make steps in values impossible.

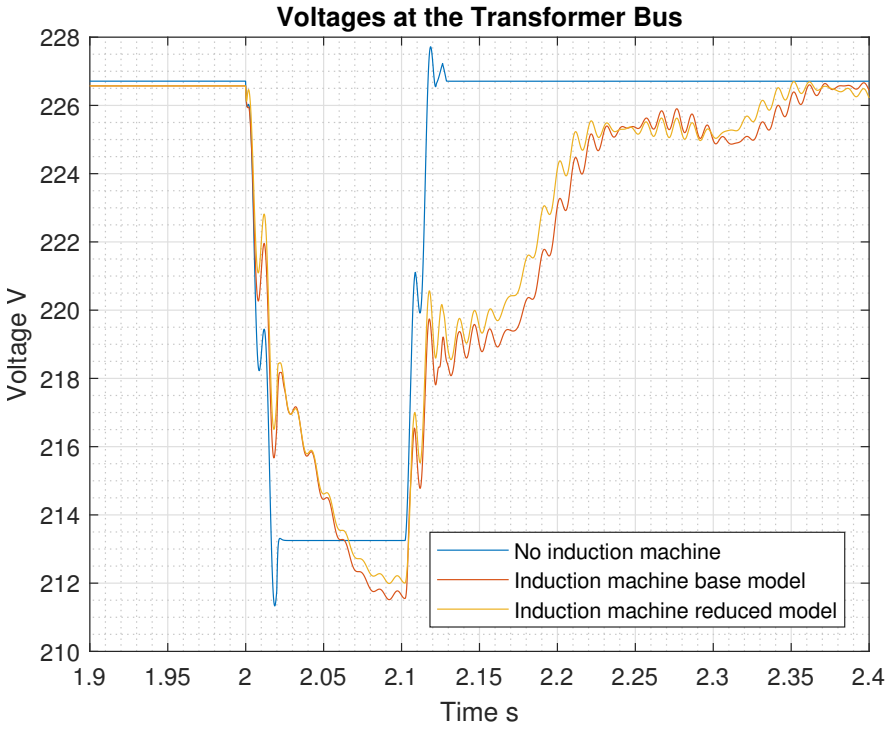

Figure 6.3: Comparison of Voltages at the Transformer Bus

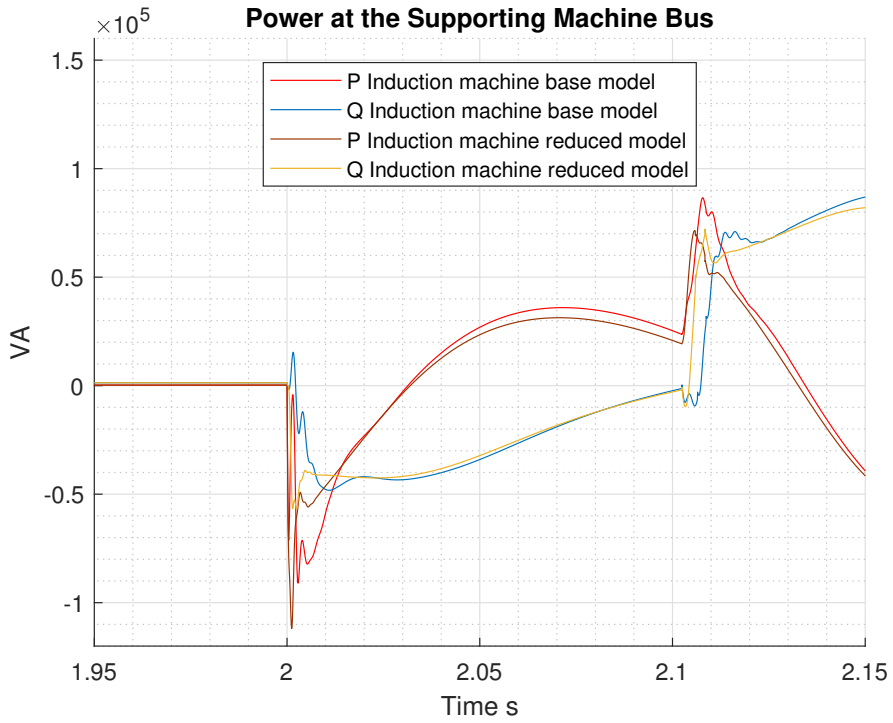

Figure 6.4: Comparison of currents at the Supporting Machine Bus

Figures 6.5 and 6.6 show the currents at the transformer bus and the supporting machine bus. Both machine models show very similar behaviour again, keeping the current at the transformer bus at a lower level at the first instant but then surpassing the short circuit current level of the case without a supporting machine. The reason for this are the big short circuit currents induction machines draw. Here the full model delivers a less conservative result with higher peaks in short circuit currents, which makes faults easier to detect.

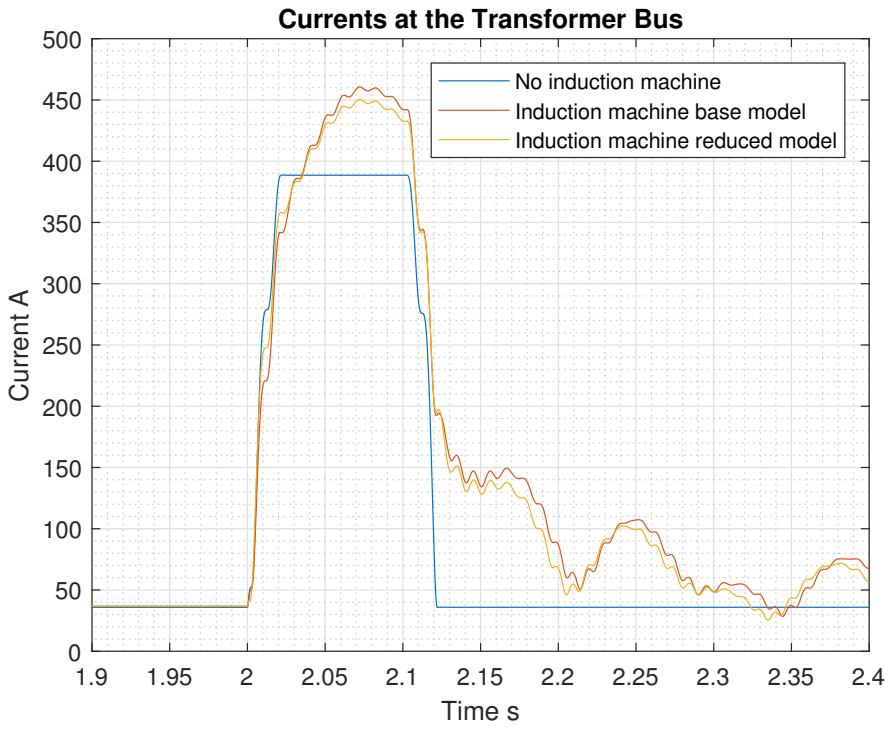

Figure 6.5: Comparison of Currents at the Transformer Bus

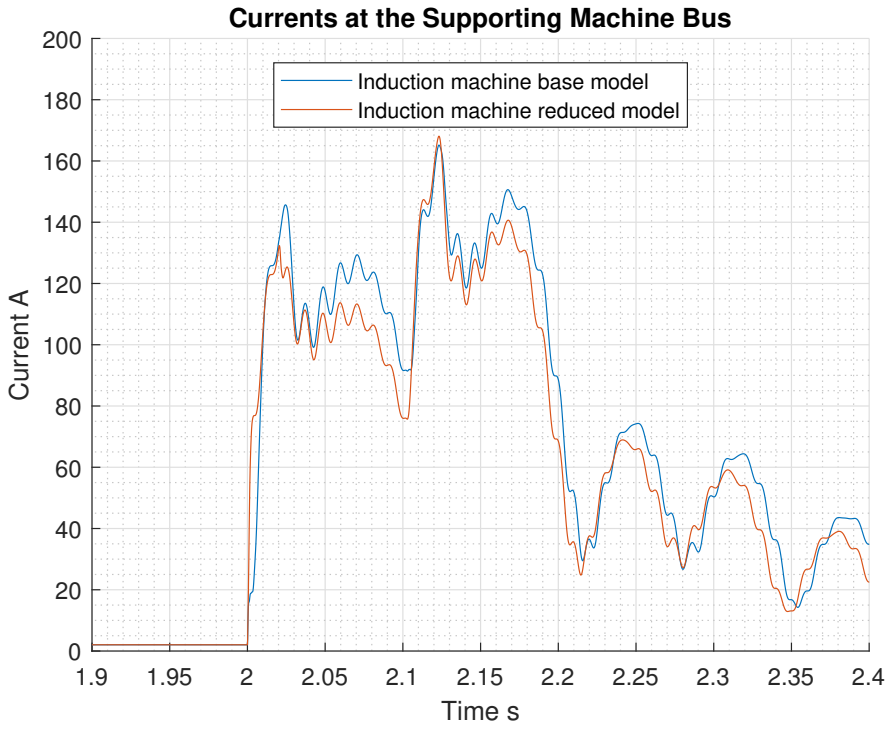

Figure 6.6: Comparison of Power at the Supporting Machine Bus

As prompted in [23] short circuit currents don't abate quickly for big low voltage induction motors. Ratios of short circuit current to no load current of > 5 are to be expected.

6.1.3 Conclusion

The Base Model provides a more accurate picture of the transient behaviour. This results in discrepancies concerning the power output in the first instant and the initial voltage dip during motor start-up. As far as the short circuit is concerned the behaviour of the system is very similar for both machine models. The full model delivers slightly higher results for the current.
Therefore, in order to be able to make more reliant predictions of the system behaviour only the base model is used in further analysis.

6.2 Comparison of Flywheel size

As a next step the motor start-up and the short circuit cases were simulated with the induction machine base model with an enlarged inertia as a supporting machine. This was done to simulate the impact of a flywheel attached to the machine.

6.2.1 Motor Start-up

The increased inertia implies a higher amount of energy contained in the rotating mass of the supporting machine. As figure 6.7 depicts this leads to a longer lasting voltage support by the machine with the attached flywheel. Due to the mass added by the flywheel the machine decelerates slower which makes the improved behaviour possible.

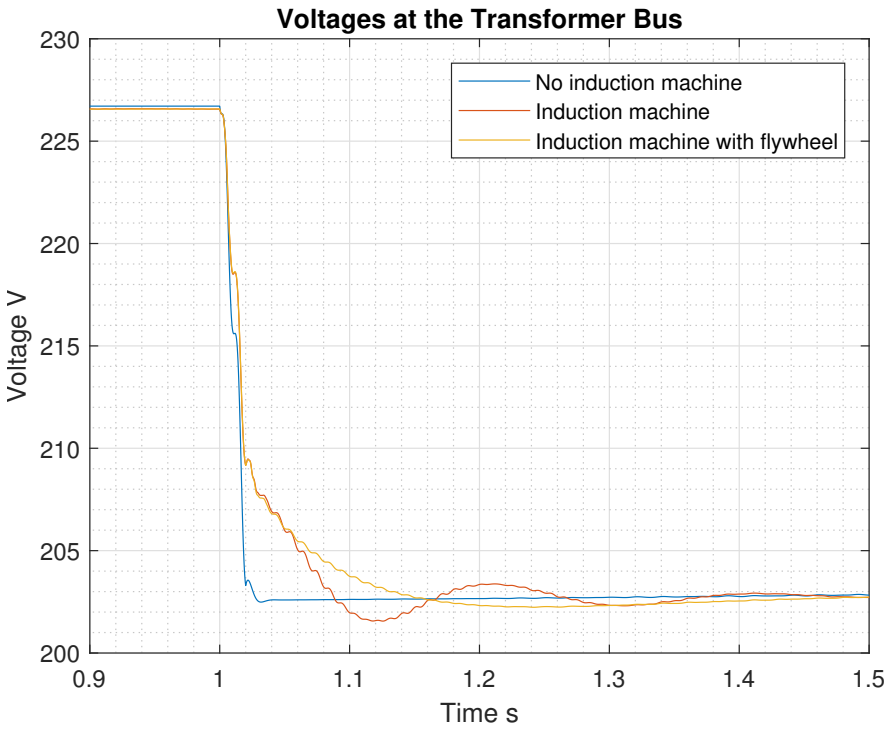

Figure 6.7: Comparison of Voltages at the Transformer Bus

Another effect of the increased inertia becomes clear in figure 6.8: both machines deflect the initial deep voltage dip, but the machine including the flywheel adds less oscillations to the voltage at the local load afterwards.

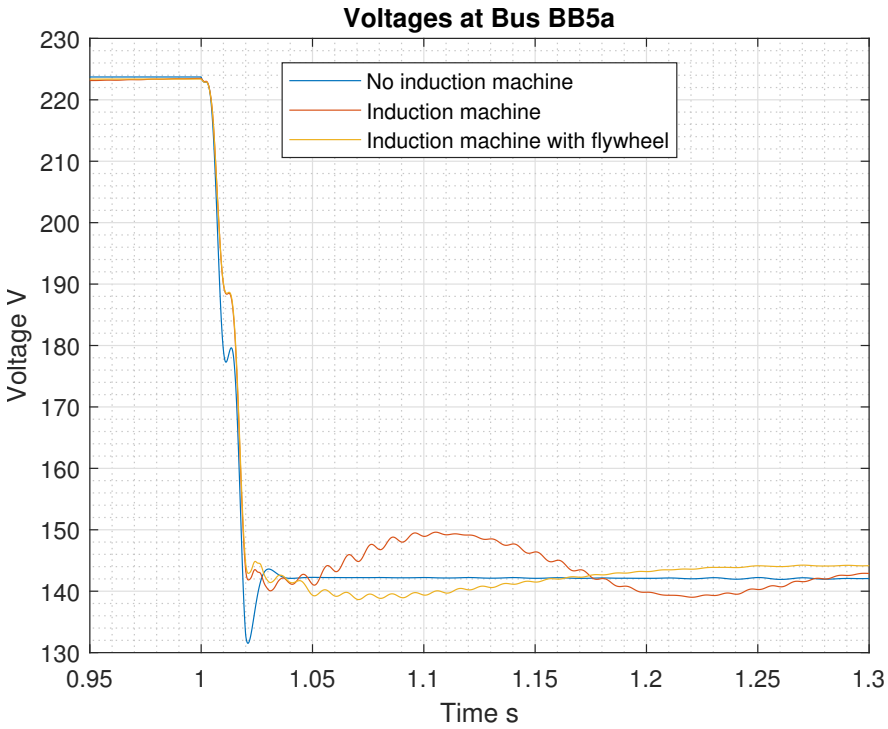

Figure 6.8: Comparison of Voltages at Bus BB5a

Figure 6.9 draws a similar picture: the current at the supporting machine bus abates almost without oscillations after the motor start-up has occurred.

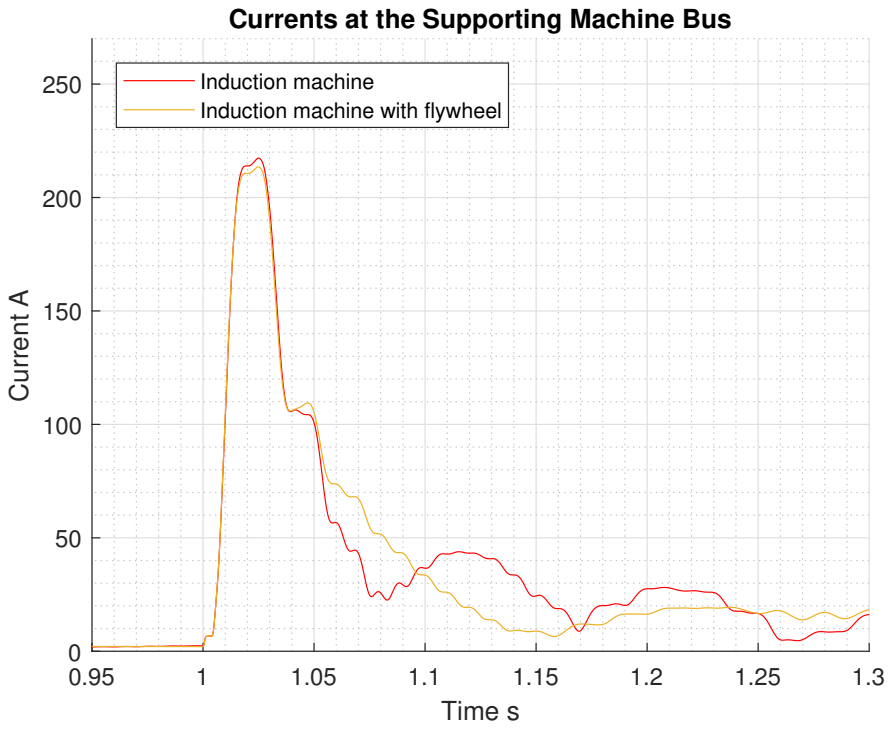

Figure 6.9: Comparison of Currents at the Supporting Machine Bus

Naturally the machine with the bigger inertia is less likely to oscillate and therefore less vulnerable to backlashes of the rest of the grid. This could help adding more stability to the grid.

6.2.2 Short Circuit

In the short circuit case the impact of the bigger inertia due to the flywheel become more striking. As figure 6.10 shows the machine including the flywheel is able to support the voltage at the transformer for a longer period of time than just the induction machine. The voltage level is sustained above the level without any support for the entire duration of the short circuit.

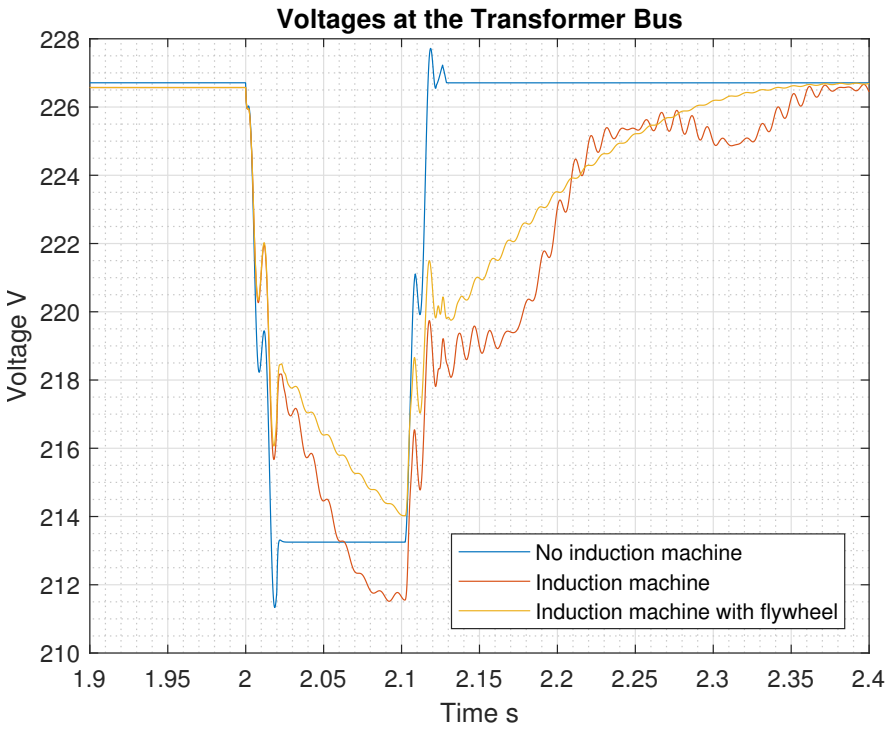

Figure 6.10: Comparison of Voltages at the Transformer Bus

Figure 6.11 depicts a similar behaviour for the local load bus BB5a. Also, here the voltage support is effective for a longer time and at a level which is above the one without any kind of support:

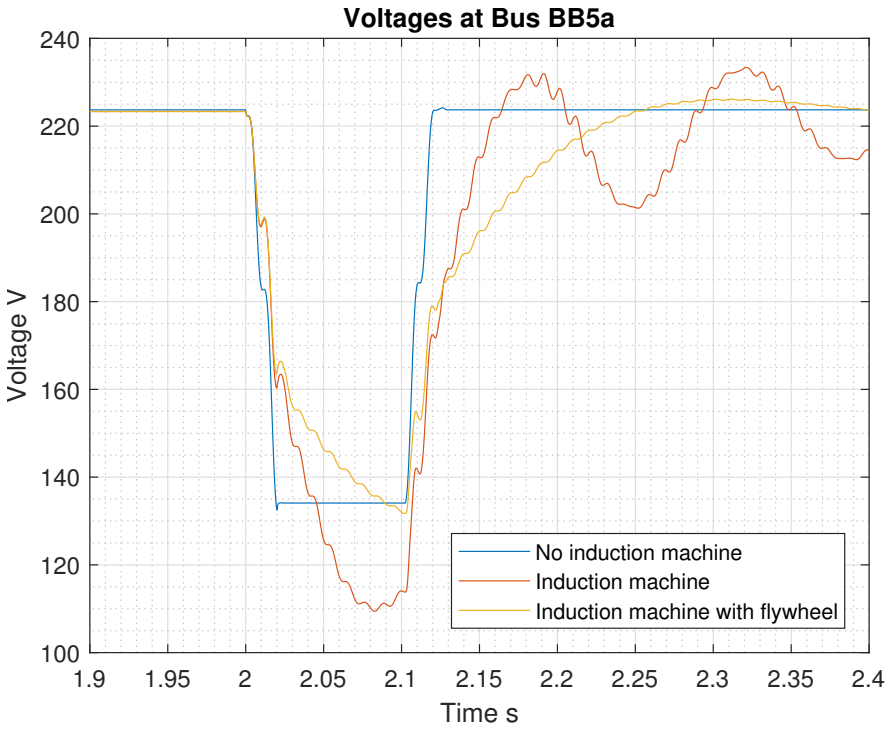

Figure 6.11: Comparison of Voltages at Bus BB5a

Due to the bigger inertia a higher rotating energy is stored, and the machine decelerates not as quickly. This improves the performance of the voltage support.

The increased inertia influences also the short circuit currents at the transformer bus. As one can see in figure 6.12 the short circuit current at the transformer bus is lower in the case of the supporting machine including the flywheel as in the case without the flywheel. Also, the short circuit currents abate quicker for the lack of oscillations than without the flywheel. The supporting machine with the flywheel keeps the current below the level without any supporting machine for more than half the duration of the short circuit and over shoots only marginally after that until the fault is cleared. This appears to be a case of blinding as described in [7]. The induction machine and the transformer feed the fault in parallel, decreasing the current from the transformer.

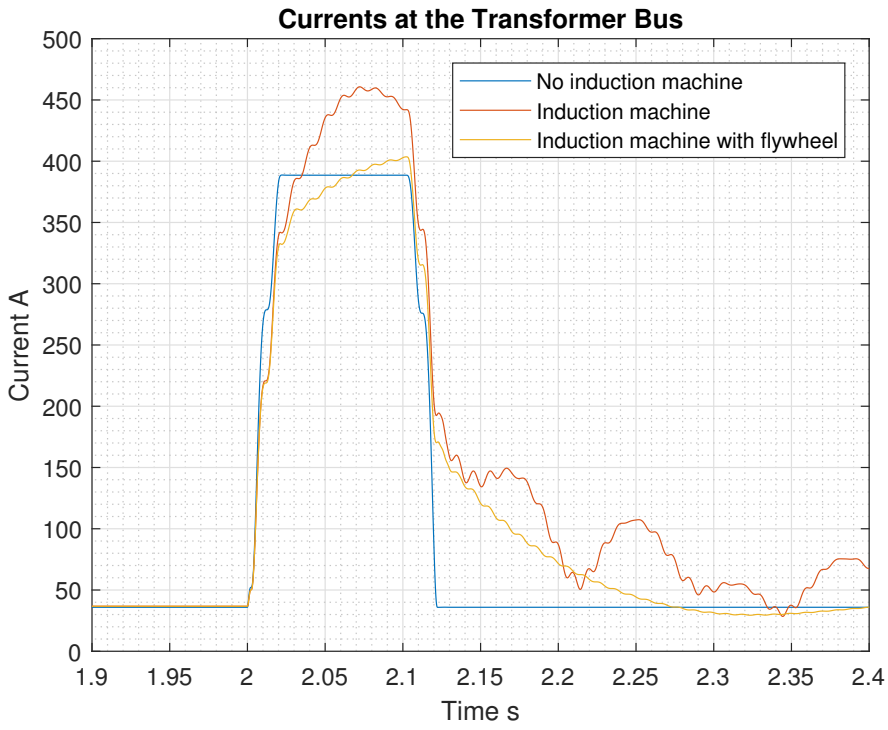

Figure 6.12: Comparison of Currents at the Transformer Bus

This behaviour can be explained by looking at the current drawn by the supporting machine in 6.13: the initial peak of short circuit current is the same for both the machine with and without the flywheel. After that the current at the supporting machine including the flywheel fades off quickly to a much lower level. Also, oscillations do not occur in the current curve.

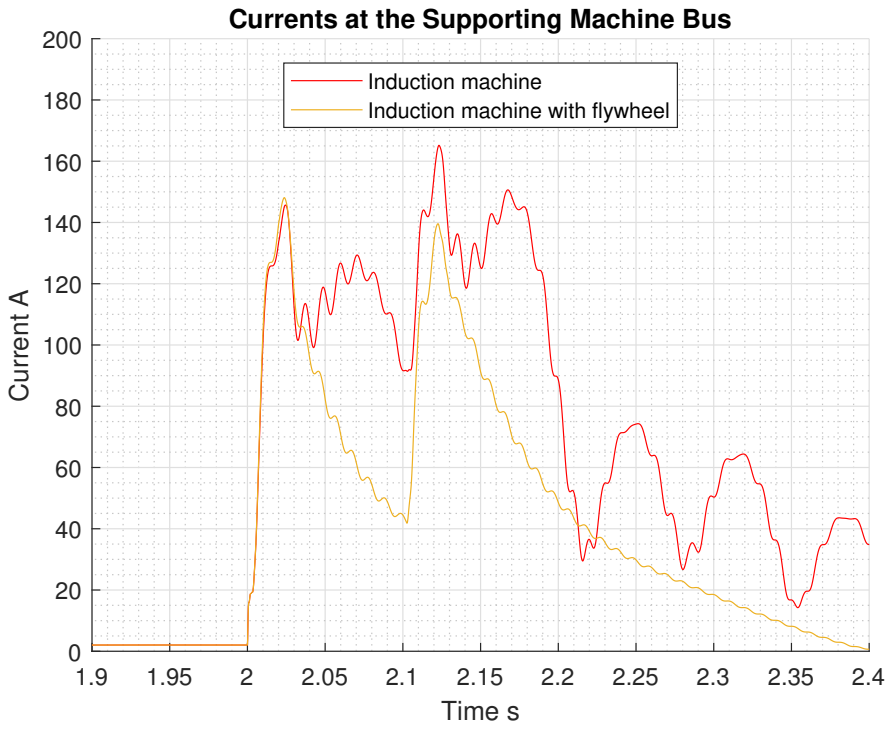

Figure 6.13: Comparison of Currents at the Supporting Machine Bus

At the local load the supporting machine with the flywheel achieves a more favourable current curve. The current is kept above the level without support for the entire short circuit, as can be seen in 6.14 In combination with the improved voltage behaviour this means more power can be supplied to the local load during the short circuit as well.

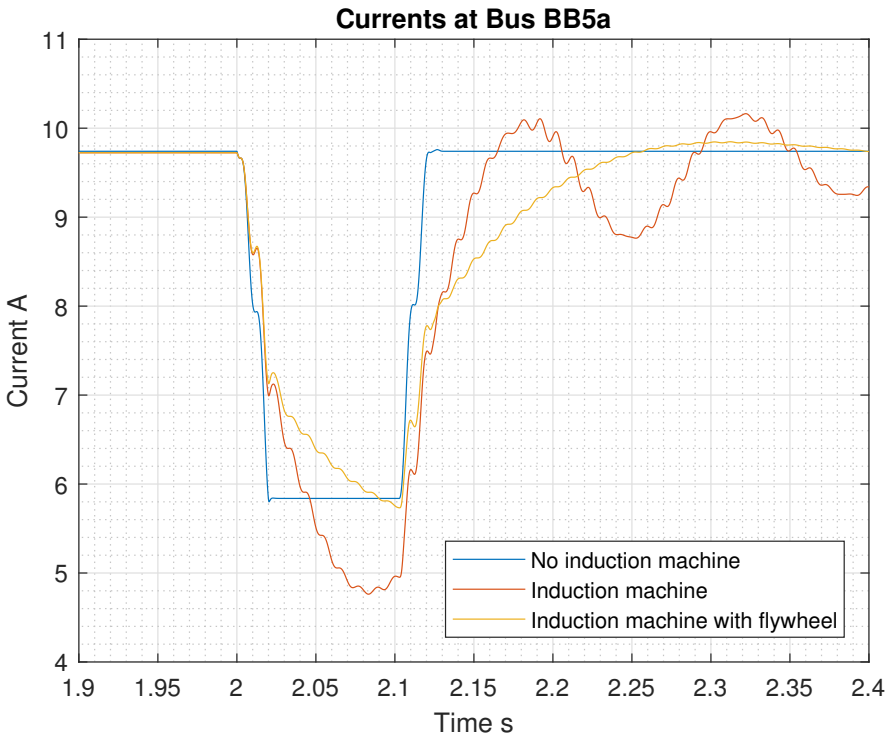

Figure 6.14: Comparison of Currents at Bus BB5a

6.2.3 Conclusion

The increased inertia introduced by the flywheel helps to support the voltage more lasting. Especially during short circuit this solution is advantageous to boost the voltage. The short circuit currents are damped at the transformer which can pose a problem for protection concerning the traceability of faults. More current is provided to the local load during the short circuit which can help to avoid sudden power outages.
Due to these outweighing advantages the supporting machine with the flywheel is used in the following.

6.3 Comparison of Induction Machine and Synchronous Machines

In this last step the most favourable solution of the simulations above, the induction machine base model with attached flywheel, is compared to two types of synchronous machines: a PMSM and a electrically excited synchronous machine. The PMSM is a synchronous machine used frequently for flywheel applications and therefor examined as a solution.The electrically excited synchronous machine is widely used to provide electrical energy which is why this machine are used as a reference.

6.3.1 Motor Start-up

At the motor start-up the three examined solutions differ in the improvement delivered.
At the transformer bus, as pointed out before, the induction machine solution supports the voltage for a short while. Also, the electrically excited synchronous machine shows this behaviour, but only to a smaller extent and for a short period of time. The voltage level quickly drops beneath the level without any supporting machine. The PMSM does not provide significant voltage support at all at the transformer bus. This can be seen in figure 6.15:

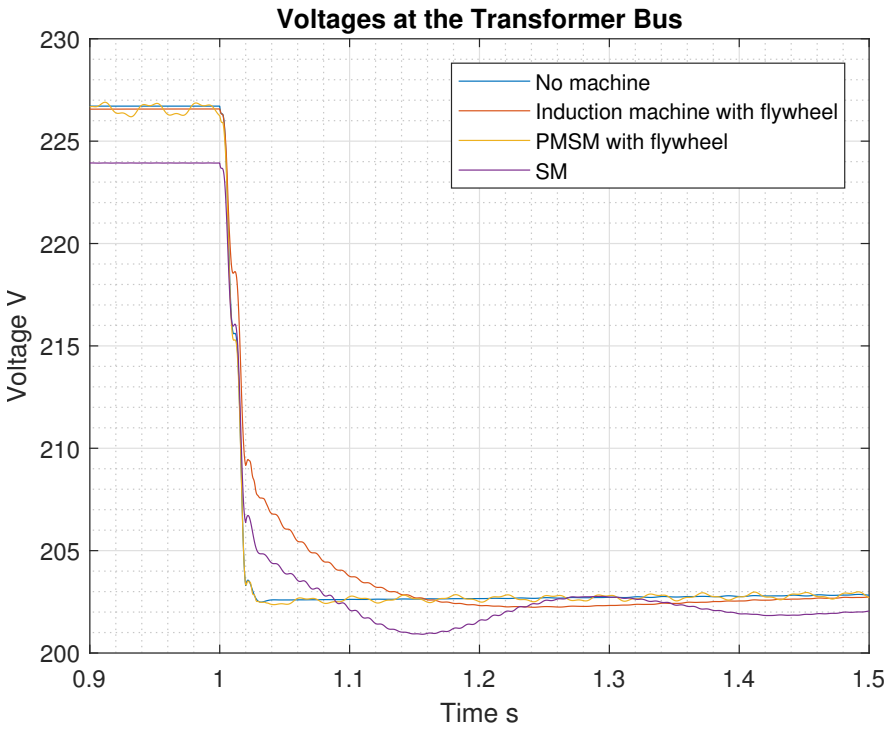

Figure 6.15: Comparison of Voltages at the Transformer Bus

At the local load the induction machine with flywheel bolsters the initial deepest voltage sag. Both the electrically excited synchronous machine and the PMSM do not provide this sort of voltage support. Only a very small improvement towards the case without any supporting machine is notable. The synchronous machine stabilizes the voltage at a level that is closer than the initial one to the level without any support but pushes the voltage down after the initial voltage sag. The synchronous machine only lifts the voltage above the level without any support for a very short time. The PMSM introduces oscillations in the voltage. Figure 6.16 illustrates this:

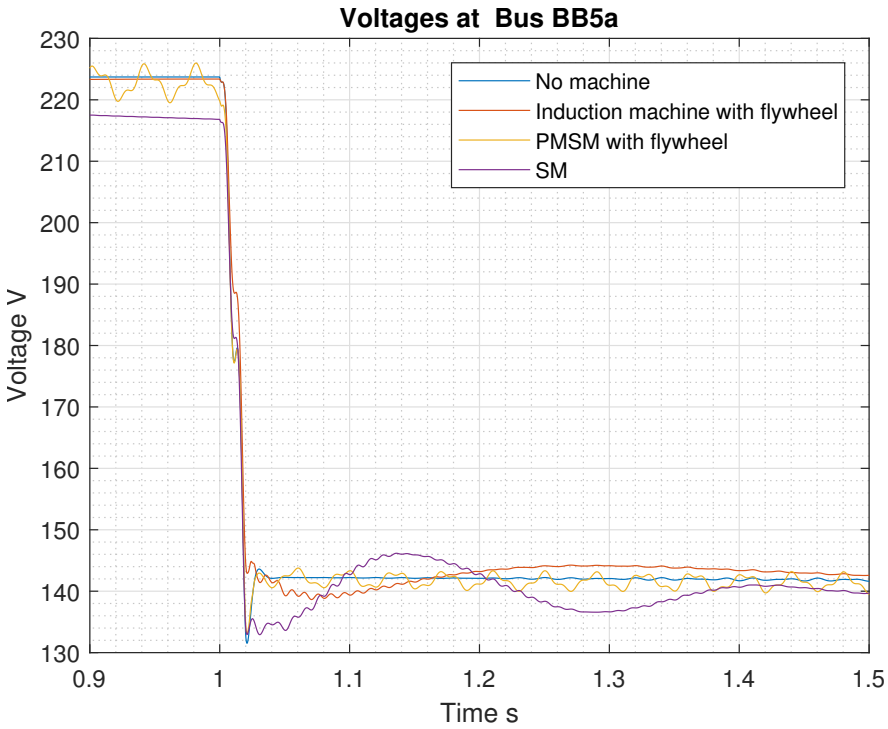

Figure 6.16: Comparison of Voltages at Bus BB5a

Figure 6.17 makes clear why this behaviour is observed: the induction machine provides the most reactive power in the first instant, the electrically excited synchronous machine less and the PMSM almost none. Also, the induction machine provides reactive power for a longer period of time. Therefor the induction machine is able to support the voltage better than the two other machines, and especially avoid the voltage dip at the begin of the start-up. Nevertheless, the synchronous machine provides active power for a short time 100ms after the start-up. This lifts the voltage at the local load as seen above. The PMSM shows oscillations in power before and after the start-up occurs, which is the cause for the oscillations it introduces in the voltage at the local load.

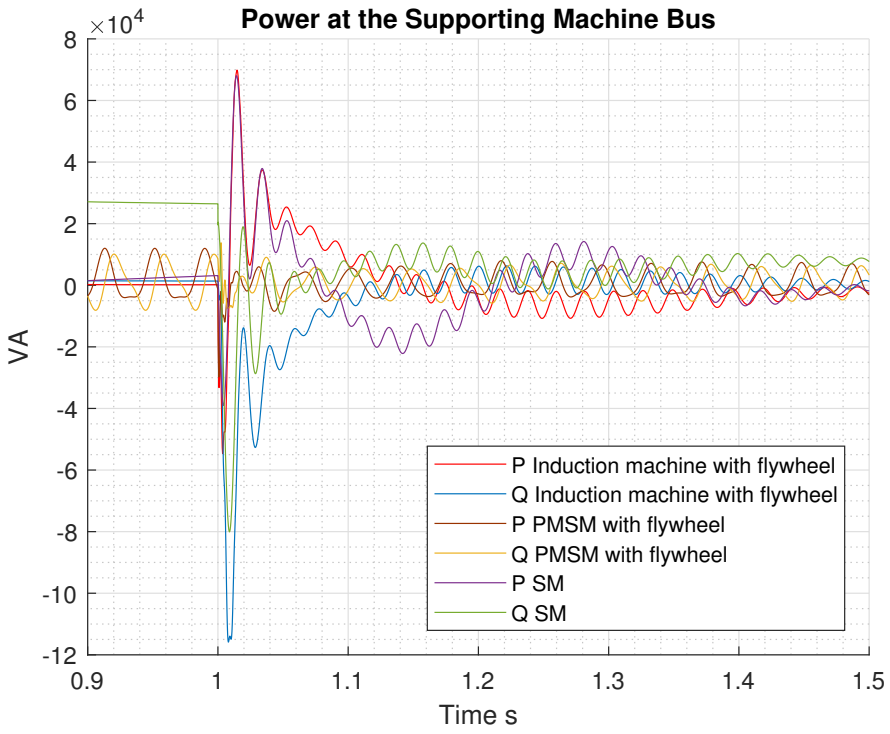

Figure 6.17: Comparison of Power at the Supporting Machine Bus

6.3.2 Short Circuit

In the short circuit case all machines deliver differently well as figure 6.18 shows: again as showed above the induction machine keeps the voltage at the transformer bus above the level without any supporting machine for the entire duration of the fault. The synchronous machine shows similar behaviour, but not being able to keep the voltage at an as high level. However, in the case of the synchronous machine the voltage at the transformer bus returns to its initial level quicker. The PMSM again does not provide voltage support, only adding minor fluctuations in the voltage.

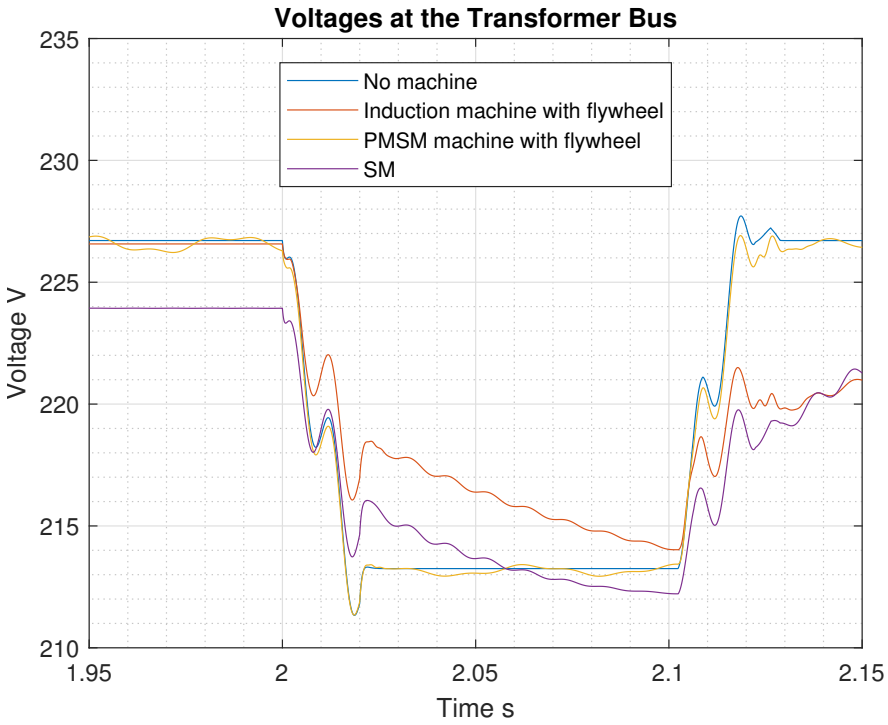

Figure 6.18: Comparison of Voltages at the Transformer Bus

This can once again be explained by looking at the power at the supporting machine bus shown in 6.19: the induction machine gives off both active and reactive power. The electrically excited synchronous machine also feeds power back to the grid but not in as big quantities. Also, the power provided diminishes quicker for the synchronous machine. The PMSM once again does not significantly provide power to the grid during the fault, which explains its lack of effect.

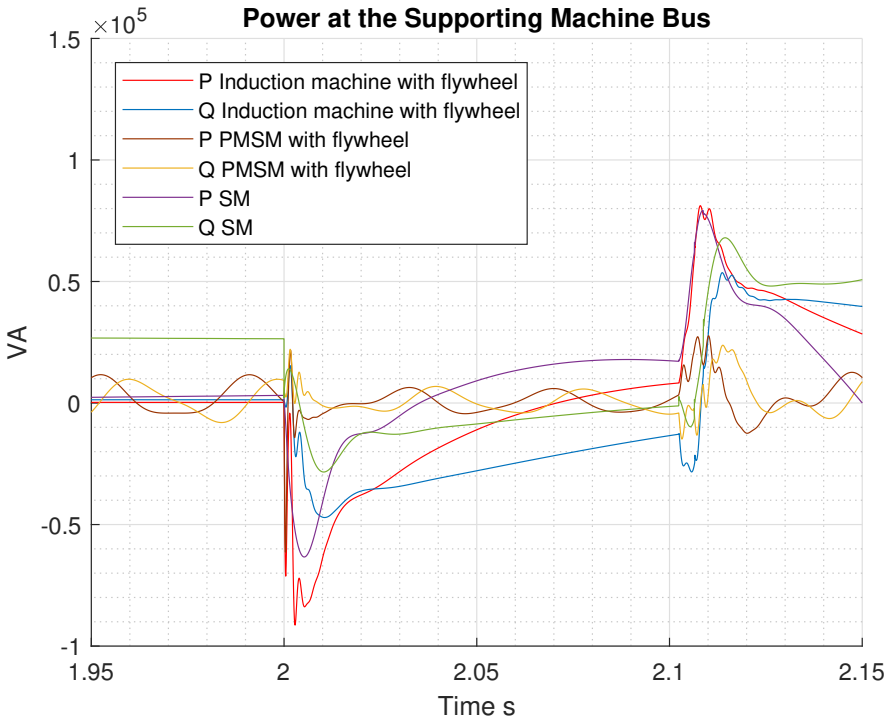

Figure 6.19: Comparison of Power at the Supporting Machine Bus

The short circuit current at the transformer bus in figure 6.20 shows a similar picture. The induction machine as supporting machine keeps the current below the level without any support for most of the fault duration. The electrically excited synchronous machine only has this effect in the very first moments of the short circuit. Then the current surpasses the value without any support. As indicated in [7] both the synchronous as the induction machine cause blinding to a certain degree. For both the currents only slowly return to their initial values after the fault is cleared.

This is different for the PMSM as it once again does not have great influence on the system behaviour in general. Only slight oscillations are added by it.

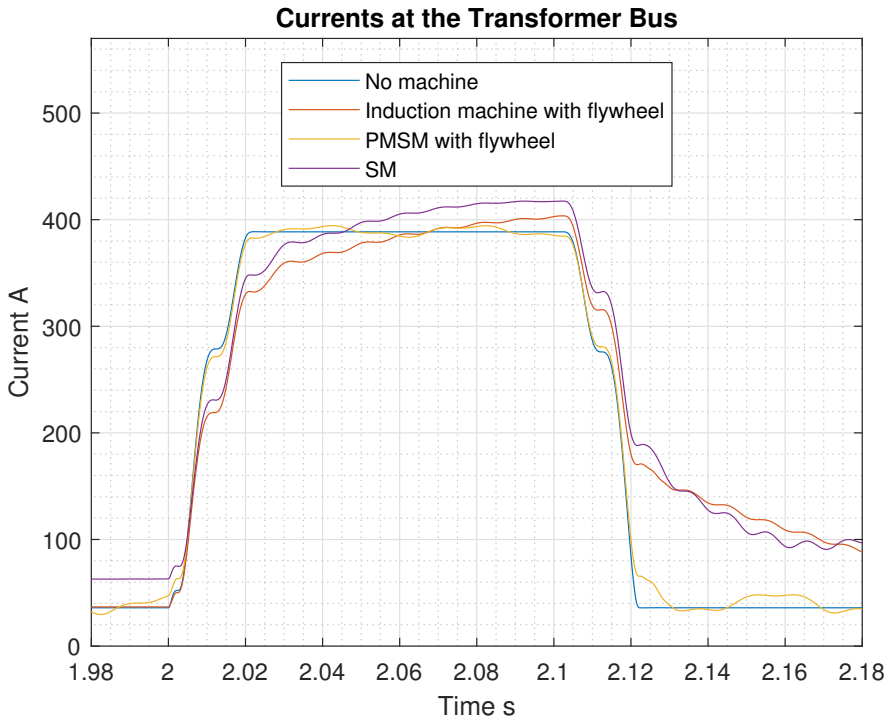

Figure 6.20: Comparison of currents at the Transformer Bus

Figure 6.21 shows how different the currents at the various machines are: the PMSM has only a small peak in current as the short circuit occurs. The electrically excited synchronous machine has a more significant peak in current, which then returns to its initial value quickly. Only the induction machine maintains a high current for a longer period of time after the initial peak. This enables the induction machine to provide short circuit current to feed into the short circuit. Therefore, the current fed into the fault by the transformer is diminished as discussed above.

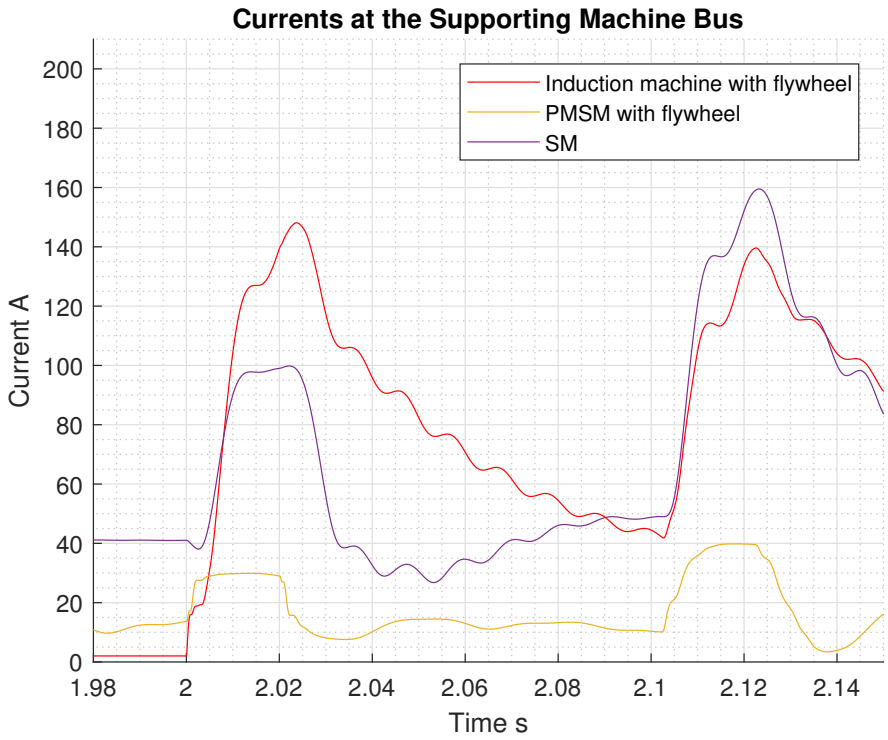

Figure 6.21: Comparison of Currents at the Supporting Machine Bus

6.3.3 Conclusion

The induction machine and the electrically excited synchronous machine both enhance the voltage stability, which is especially the case for the short circuit case. The induction machine appears to be superior to the synchronous machine in voltage support, but the electrically excited synchronous machine shows better behaviour as far as short circuit currents at the transformer are concerned.

The PMSM fails to add meaningful improvements to the grid stability and only seems to introduce distortions to the voltage.

7 Discussion

In this chapter the measures implemented for stability improvement are compared and conclusions are drawn about their effectiveness. In addition to that an outlook for further possible work on this topic is given.

7.1 Discussion

As the results show the induction modelling approach neglecting stator flux derivatives, even if widely used in power system analysis, only produces simulation results of questionable accuracy concerning the transient behaviour of the system. This is especially problematic for increased loads since voltage dips are not depicted correctly, but also for faults since the full induction machine model delivers different predictions of the system response and short circuit currents.

For this analysis another point of interest was how significant the impact of a flywheel attached to the supporting machine is. The simulations point out that the flywheel adds increased stability to the network and enables the supporting induction machine to boost the voltage for longer. Important for the short circuit case is the decrease in short circuit current at the transformer bus. Due to blinding the induction machine including the flywheel feeds more current into the fault diminishing the fault current at the transformer. This can have an impact on protection for too low currents may not be detected by protection relays [7] and should be taken into consideration when implementing such a solution. The currents fed into the grid by the machine can also lead to the machine being disconnected for no reason, because relays do not recognize the direction of the current.

Finally, an electrically excited synchronous machine and a PMSM were used for the supporting machine, each providing different grades of improvement. The electrically excited synchronous machine provides some voltage support at the transformer during the motor

start-up, even though it's transient contribution at the local load is negligible. The short circuit case draws a similar picture: the SM provides only some voltage support. Also, the electrically excited synchronous machine feeds current into the fault, causing the same potential issues as the induction machine, even if its impact is smaller in the case simulated. On the other hand, the PMSM does not provide significant voltage support or adds a notable blinding effect by feeding voltage into the fault.

To validate these results a real-life setup by TrønderEnergi tested the impact of an induction machine on the grid. An 18kVA induction machine was linked to a local load bus in a rural distribution grid in the region surrounding Trondheim. As a starting motor for the test purposes a one-phase 1.5kVA wood chopper was used, for devices like this are the most problematic as stated by the utility. Figure 7.1 shows the measurement with and without the supporting induction machine. The test qualitatively confirms the quality of the induction machine to provide voltage support in the first instant of the motor start: the initial voltage dip is reduced by roughly 3V from about 216V to 219V. There is no capacity bank in this setup which means the induction machine is implemented without any compensation. This results in a lower steady state voltage at the local load.

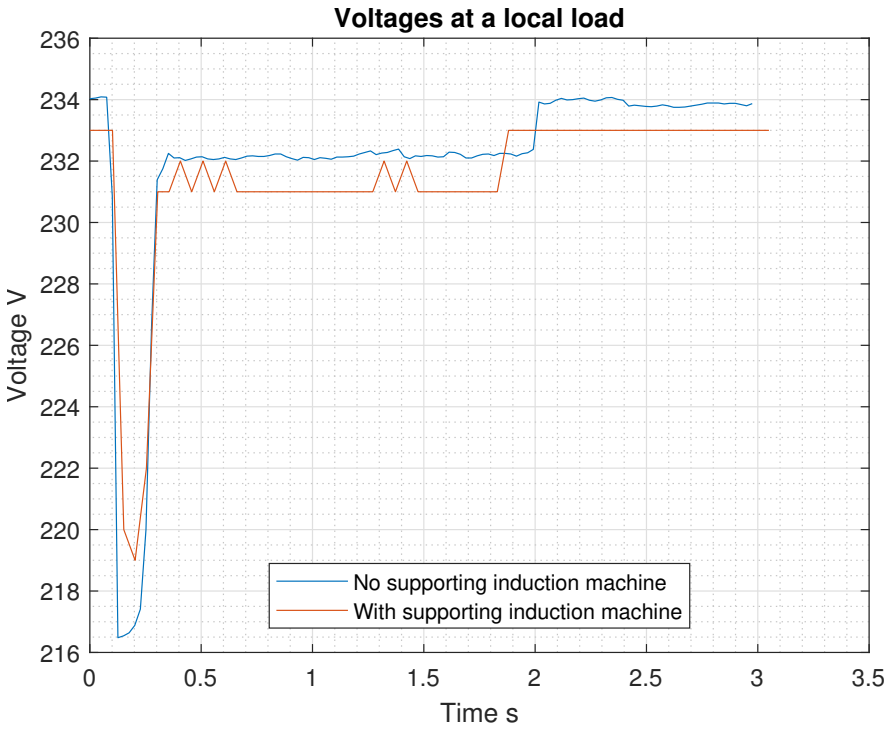

Figure 7.1: Results of measurements on a local load

7.2 Conclusion

The results for the low voltage distribution grid analysed and simulated point to the induction machine including a flywheel as the preferred mean of voltage control. This solution shows the best performance in an increased load scenario, as the motor start-up, as well as in a fault case, the 3-phase line to ground short circuit. It provides voltage support both at the transformer bus and at the local load for a limited time and especially for the transient time frame. In regard to these aspects the proposed solution shows preferable behaviour in comparison to the electrically excited synchronous machine, the PMSM and just the induction machine without a flywheel. Only the big short circuit currents fed into the fault by the induction machine including the flywheel pose a disadvantage regarding protection schemes. Protection schemes have to be in compliance with the impact of the currents for such a solution to be implemented. In addition, the full induction machine model should be used to simulate the supporting machine since it provides more conservative results.

7.3 Further work

There are several aspects in this thesis requiring further investigation.
Starting with the modelling aspect of the thesis, the cause of the discrepancy in power consumption between the custom induction machine model and the *Simscape*® built-in model remains unclear but could be brought to light. In addition, the modelling of the PMSM might be an interesting aspect to do further work on since it is not ruled out that the used PMSM model is responsible for its little effect on the grid behaviour. In addition, a control scheme could be developed for the PMSM.
Concerning the simulation, a sensitivity analysis on the placement of the supporting machine in the grid could be resourceful. An analysis like this could be conducted both for the short circuit and motor start-up case, also with respect to the the position of the fault or the increased load in the network. Furthermore, different types of faults, including non-symmetric ones, could be analysed.

Moreover, further supporting devices could be investigated. This could be especially interesting for boosting the voltage during steady state. One possible solution here is the Magtech Voltage Booster as investigated in [29]:

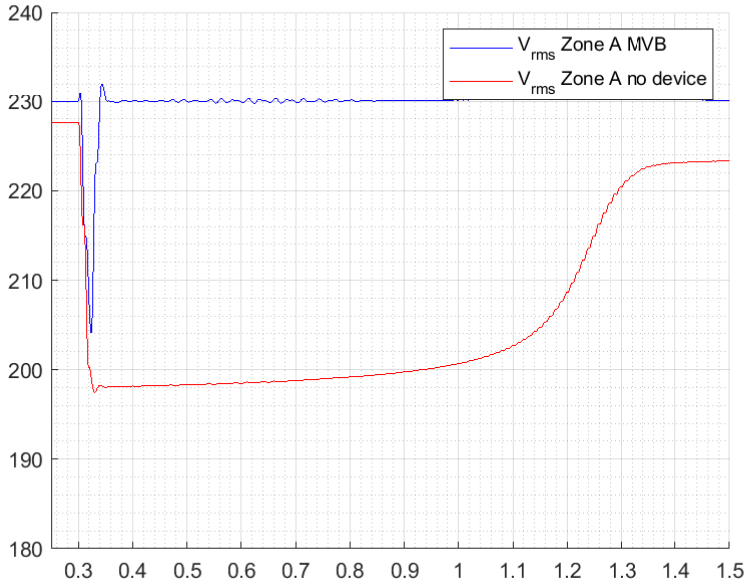

Figure 7.2: Motor start-up with a Magtech Voltage Booster

Figure 7.2 shows how the Magtech Voltage Booster improves the steady state voltage stability during the motor start-up. Nevertheless, it does not provide any support in the first instant. This points to a combination of the voltage booster and a supporting machine to be of interest for further investigation.

Bibliography

[1] R. Gloor, "Energiesparmöglichkeiten in sägereien," Bundesamt für Konjunkturfragen, Report, 1996.

[2] H. M. Chou and K. L. Butler-Purry, "Investigation of voltage stability in unbalanced distribution systems with dg using three-phase current injection based cpf," in *2014 IEEE PES General Meeting — Conference Exposition*, July 2014, pp. 1–5.

[3] K. Kawabe, T. Nanahara, and K. Tanaka, "Importance of considering induction motor load for studying impact of photovoltaic generation on transient stability of power systems," in *2017 IEEE Manchester PowerTech*, June 2017, pp. 1–6.

[4] S. KATO, T. TAKAKU, H. SUMITANI, and R. SHIMADA, "Development of voltage sag compensator and ups using a flywheel induction motor and an engine generator," *Electrical Engineering in Japan*, vol. 167, no. 1, Feb. 2009.

[5] G. CIMUCA, M. M. RADULESCU, C. SAUDEMONT, and B. ROBYNS, "Losses and efficiency of a flywheel energy storage system with permanent-magnet synchronous machine associated to a variable-speed wind generator," Apr. 2018.

[6] A. Anwar, N. K. Roy, and H. R. Pota, "Voltage stability analysis with optimum size and location based synchronous machine dg," in *AUPEC 2011*, Sept 2011, pp. 1–5.

[7] K. Mäki, S. Repo, and P. Järventausta, "Protection coordination to meet the requirements of blinding problems caused by distributed generation," vol. 4, pp. 674–683, 07 2005.

[8] *Radial Topology*, TrondEnergy, 3 2018.

[9] "Matlab simscape," 2017b, the MathWorks, Natick, MA, USA.

[10] S. Barker, S. Kalra, D. Irwin, and P. Shenoy, "Empirical characterization, modeling, and analysis of smart meter data," *IEEE Journal on Selected Areas in Communications*, vol. 32, no. 7, pp. 1312–1327, July 2014.

[11] A. J. Schwab, *Elektroenergiesysteme*. Berlin Heidelberg: Springer, 2009.

[12] ABB, "Distribution transformers," Data sheet, 2000.

[13] K. Uhlen, "Modelling and robust control of autonomous hybrid power systems," The University of Trondheim, The Norwegian Institute of Technology, Report, 1994.

[14] P. Krause, O. Wasynczuk, and S. Sudhoff, *Analysis of Electrical Machinery and Drive Systems*. Wiley-Interscience, 2002.

[15] P. Kundur, *Power System stability and control*. New York San Francisco: McGraw-Hill, Inc., 1993.

[16] T. Van Cutsem, "Dynamics of the induction machine," Lecture Slides, 2017.

[17] M. I. L. Marques, "Design and control of an electrical machine for flywheel energy-storage system," Instituto Superior Tecnico, Report, 2008.

[18] A. Binder, *Elektrische Maschinen und Antriebe*. Berlin Heidelberg: Springer, 2012.

[19] R. Fischer and H. Linse, *Elektrotechnik für Maschinenbauer*. Wiesbaden: Springer Fachmedien, 2012.

[20] Rasjonell Elektrisk Nettvirksomhet, "Distribusjonsnett – tekniske verdier," Data sheet, 2011.

[21] R. D. Zimmerman, C. E. Murillo-Sánchez, and R. J. Thomas, "Matpower: Steady-state operations, planning and analysis tools for power systems research and education," *Power Systems, IEEE Transactions on*, vol. 26, no. 1, Feb. 2011.

[22] Y. Narkhede, "Simscape modeling of motor-generator unit components for hybrid eleectric vehicle," Georgia Insitute of Technology, Report, 2016.

[23] D. Oeding and B. R. Oswald, *Elektrische Kraftwerke und Netze*. Berlin Heidelberg: Springer, 2011.

[24] C. Alacs, "Lva 370.029 - seminar energieversorgung," Lecture Script, 2017.

[25] R. NATARAJAN and J. WANG, "Estimation of synchronous machine parameters from performance relations," *Electric Power Systems Research*, vol. 20, 1991.

[26] E. Schrüfer, L. Reindl, and B. Zagar, *Elektrische Messtechnik*. München: Carl Hanser Verlag, 2012.

[27] S. Miller, "Modeling physical systems as physical networks with the simscape language," Handbook, 2008.

[28] M. Wurm, "Skriptum zur lu 370.024:schutztechnik," Lecture Script, 2017.

[29] A. Karoui, "Short circuit capacity improvement techniques for a low voltage distribution grid," NTNU, Norges teknisk-naturvitenskapelige universitet, Report, 2018.